

## The Borel Regulator Map on Pictures, II: An Example from Morse Theory

KIYOSHI IGUSA\*

*Department of Mathematics, Brandeis University, Waltham, MA 02254-9110, U.S.A.*

and

JOHN KLEIN

*Fakultät für Mathematik, Universität Bielefeld, Universitätsstr., 4800 Bielefeld, Germany*

(Received: November 1991)

**Abstract.** By doing parametrized Morse theory on circle bundles over  $S^2$ , we produce ‘pictures’ representing elements of  $K_3$  of cyclotomic number fields. By computing the regulator map on these pictures, we show that they are rationally nontrivial.

**Key words.** Algebraic  $K$ -theory, dilogarithm, Morse theory, pseudoisotopy.

### 0. Introduction

In Part I, we gave a formula for the Borel regulator map  $b: K_3\mathbb{C} \rightarrow \mathbb{R}$  on elements of  $K_3\mathbb{C}$  represented by pictures. In Part II, we will simplify this formula so that it is effectively computable, we will construct explicit pictures  $L_n$  (Figure 2.3 in Part A) representing elements of  $K_3\mathbb{Z}[\xi]$ , where  $\xi$  is any nontrivial  $n$ th root of unity and we will show that  $b(L_n) = n \operatorname{Im} \operatorname{dilog}(\xi)$ .

The pictures  $L_n$  were obtained by doing parametrized Morse theory on circle bundles over  $S^2$ . The idea is very simple. A circle bundle  $S^1 \rightarrow E \rightarrow S^2$  is basically a family of circles parametrized by  $S^2$ . Any generic smooth function  $f: E \rightarrow \mathbb{R}$  gives a Morse function on almost every fiber. Each such Morse function produces an incidence matrix with coefficients in  $\mathbb{Z}[\pi_1 E]$  and the determinant of this matrix will be  $1 - u$ , where  $u$  is the generator of  $\pi_1 E = \mathbb{Z}/n$ . If  $n \geq 2$ , then we can map  $u$  to  $\xi \in \mathbb{Q}[\xi]$ , these matrices will become invertible and we will get a two parameter family of invertible matrices. Over a one-dimensional subset of  $S^2$ , the restriction of  $f$  to the corresponding fiber will not be a Morse function. This means that the matrix changes along this one-dimensional set. In fact it changes by certain elementary row and column operations uniquely specified by the principles of Morse theory. This gives us a ‘generalized picture’ representing an element of  $K_3\mathbb{Q}[\xi]$ . (Figure 5.5 in Part B.) If  $f$  is chosen to be a particularly nice function called a fiberwise positively

\* Research supported by NSF Grant No. MCS-90-02512.

oriented generalized Morse function (PGMF), then this element of  $K_3\mathbb{Q}[\xi]$  will be uniquely determined.

Our formula for the Borel regulator map works only for 'pictures' which are two-parameter families of invertible matrices which are only allowed to change by *column* operations along a one-dimensional subset of the parameter space  $S^2$ . Therefore we 'exchange' all the row operations in this generalized picture to column operations. This produces the picture  $L_n$ .

This construction is a special case of the higher Reidemeister torsion invariant defined in [11, 12]. The general situation is that there is a smooth bundle  $E$  over an even-dimensional sphere  $S^{2n}$  and a unitary representation of  $\pi_1 E$  with respect to which each fiber becomes acyclic. Then a fiberwise 'framed' function on  $E$  gives a family of acyclic chain complexes over  $\mathbb{C}$  parametrized by  $S^{2n}$ . This gives an element of  $K_{2n+1}\mathbb{C}$  modulo some indeterminacy. However, if we apply the Borel regulator map  $b_n: K_{2n+1} \rightarrow \mathbb{R}$ , we get a well-defined real valued invariant of the bundle  $E \rightarrow S^{2n}$  which is called the *higher Reidemeister torsion*, since it agrees with the usual Reidemeister torsion of  $E$  (actually the difference between the torsions of the two components) in the case when  $n = 0$ . This will be explained in greater detail in [10].

This paper is divided into two parts. In Part A we simplified the formula for the Borel regulator map and we do explicit computations on the pictures  $L_n$ . In Part B we explain how these pictures were obtained by parametrized Morse theory on circle bundles.

## PART A: COMPUTATION OF THE BOREL REGULATOR MAP ON THE PICTURES $L_n$

### 1. Computation of the Functions $p$ and $l$

In order to actually compute the Borel regulator map on any given picture, we need a better formula for the function  $p$  which was defined in Part I as an integral of the Bloch–Wigner function  $D_2$ . In this section, we will show how both  $p$  and the related function  $l$  can be computed.

We recall that by the stability properties of  $p$  and  $l$  (A2.2(e) and B1.3(d) in Part I) we can always reduce to the problem of computing:

$$pS(x, y, z), \text{ where } x, y, z \text{ are three noncollinear projective points in } P^2(\mathbb{C}), \quad (1)$$

$$l(x, y, z), \text{ where } x, y, z \text{ are distinct projective points in } P^1(\mathbb{C}). \quad (2)$$

We recall that in these dimensions  $l(x, y, z)$  is defined to be the average value of  $D_2 r(w, x, y, z)$  as  $w$  varies over all points in  $P^1(\mathbb{C})$  and  $p(L_1, L_2, L_3)$  is defined to be the average value of

$$D_2 r(L_0, L \cap L_1, L \cap L_2, L \cap L_3),$$

where  $(L_0, L)$  runs over all point-line pairs in  $P^2(\mathbb{C})$ . We also recall that  $S(x, y, z) = (\overline{xy}, \overline{yz}, \overline{xz})$  where  $\overline{ab} = \text{span}(a, b)$ .

The computation is based on the fact that the Bloch–Wigner function satisfies the following elementary identity:

$$D_2(\bar{z}) = -D_2(z). \quad (3)$$

In particular,  $D_2(z) = 0$  if  $z$  is real. It is easy to see that the functions  $p$  and  $l$  inherit this property. Thus, we get the following lemma.

LEMMA 1.1.

- (a)  $pS(\bar{x}, \bar{y}, \bar{z}) = -pS(x, y, z)$ ,
- (b)  $l(\bar{x}, \bar{y}, \bar{z}) = -l(x, y, z)$ ,

where, e.g.,  $\bar{x}$  is given by conjugating all the coordinates of  $x$ . □

LEMMA 1.2.

- (a)  $pS(x, y, z) = 0$  if any two of the vectors  $x, y, z$  are perpendicular.
- (b)  $l(x, y, z) = 0$  if any two of the vectors  $x, y, z$  are perpendicular.

*Proof.* In both cases, there is a unitary transformation  $g$  so that  $gx, gy, gz$  have all real coordinates. By Lemma 1.1, this forces the values of  $p$  and  $l$  to be zero. □

Let  $x, y, z$  be three points in  $P^2(\mathbb{C})$  which are not collinear and so that no two are orthogonal. Then the projective lines  $\overline{yz}, \overline{xy}, \overline{xz}$  meet the orthogonal complement  $x^\perp$  of  $x$  in three points  $a, b, c$  respectively (see Figure 1.3).

THEOREM 1.4.  $pS(x, y, z) = l(a, y, z) - l(a, b, c)$ .

*Proof.* By Proposition 3.7 in Part IA, we have

$$pS(x, y, z) + pS(x, a, y) + pS(x, z, a) = l(a, y, z) - l(\overline{xa}, \overline{xb}, \overline{xc}),$$

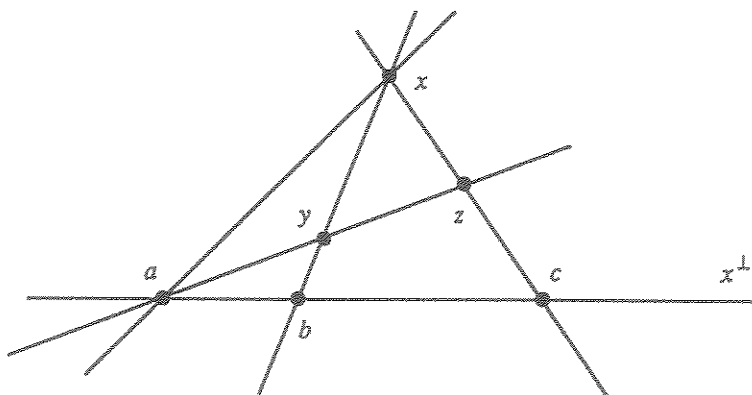


Fig. 1.3.

but  $pS(x, a, y) = 0 = pS(x, z, a)$  by Lemma 1.2 and

$$l(\overline{xa}, \overline{xb}, \overline{xc}) = l(a, b, c)$$

by the stability of  $l$  (Proposition 3.3(d) in Part IA).  $\square$

One consequence of this is the following stronger version of Lemma 1.2(a).

**COROLLARY 1.5.**  $pS(x, y, z) = 0$  if any two of the projective lines  $\overline{xy}$ ,  $\overline{yz}$ ,  $\overline{xz}$  are perpendicular.

*Proof.* Suppose that  $\overline{xy}$  and  $\overline{yz}$  are perpendicular. Then each projective line contains the orthogonal complement of the other so in the formula  $pS(x, y, z) = l(a, y, z) - l(a, b, c)$  of Theorem 1.4 we have that  $a = x^\perp \cap \overline{yz}$  is the orthogonal complement of  $\overline{xy}$ . Consequently,  $a$  is orthogonal to both  $y$  and  $b = x^\perp \cap \overline{xy}$  so both  $l$  terms vanish by Lemma 1.2(b).  $\square$

The computation of  $pS(x, y, z)$  has now been reduced to the computation of the function  $l$ .

**LEMMA 1.6.** Suppose that  $a, b, c$  are distinct points in  $P^1(\mathbb{C})$ . Then

$$l(a, b, c) - l(a^\perp, b, c) = D_2r(a^\perp, a, b, c).$$

*Proof.* It follows from the 5-point identity for  $D_2r$  that

$$D_2r(a^\perp, a, b, c) = l(a, b, c) - l(a^\perp, b, c) + l(a^\perp, a, c) - l(a^\perp, a, b).$$

But, by Lemma 1.2, the last two terms are zero.  $\square$

**LEMMA 1.7.** For any three points  $a, b, c$  in  $P^1(\mathbb{C})$  we have  $l(a, b, c) = -l(a^\perp, b^\perp, c^\perp)$ .

*Proof.* It follows from (3) that  $l(a, b, c) = -l(\bar{a}, \bar{b}, \bar{c})$ . But the unitary matrix

$$\begin{pmatrix} 0 & 1 \\ -1 & 0 \end{pmatrix}$$

transforms  $\bar{a}, \bar{b}, \bar{c}$  into  $a^\perp, b^\perp, c^\perp$ , respectively, so  $l(\bar{a}, \bar{b}, \bar{c}) = l(a^\perp, b^\perp, c^\perp)$ .  $\square$

**THEOREM 1.8.** For any three distinct points  $a, b, c$  in  $P^1(\mathbb{C})$  we have

$$6l(a, b, c) = 2D_2r(a^\perp, a, b, c) + 2D_2r(b^\perp, b, c, a) + 2D_2r(c^\perp, c, a, b) + D_2r(b^\perp, b, c, a^\perp) + D_2r(c^\perp, c, a, b^\perp) + D_2r(a^\perp, a, b, c^\perp)$$

*Proof.* By Lemmas 1.6 and 1.7, we see that

$$2D_2r(a^\perp, a, b, c) = 2l(a, b, c) - 2l(a^\perp, b, c),$$

$$2D_2r(b^\perp, b, c, a) = 2l(a, b, c) - 2l(b^\perp, c, a),$$

$$2D_2r(c^\perp, c, a, b) = 2l(a, b, c) - 2l(c^\perp, a, b),$$

$$D_2r(b^\perp, b, c, a^\perp) = l(b, c, a^\perp) - l(b^\perp, c, a^\perp) = l(a^\perp, b, c) + l(c^\perp, a, b),$$

$$D_2r(c^\perp, c, a, b^\perp) = l(c, a, b^\perp) - l(c^\perp, a, b^\perp) = l(b^\perp, c, a) + l(a^\perp, b, c),$$

$$D_2r(a^\perp, a, b, c^\perp) = l(a, b, c^\perp) - l(a^\perp, b, c^\perp) = l(c^\perp, a, b) + l(b^\perp, c, a).$$

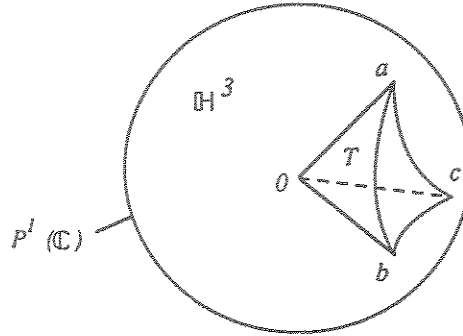
The right-hand terms all cancel, except for  $6l(a, b, c)$ .  $\square$

This formula was obtained from the following geometric interpretation of the function  $l(a, b, c)$ .

**PROPOSITION 1.9.** *If  $a, b, c$  are three distinct points in  $P^1(\mathbb{C})$ , then*

$$l(a, b, c) = \text{vol}(T_{0abc}),$$

where  $T_{0abc}$  is the ideal tetrahedron in hyperbolic 3-space  $\mathbb{H}^3$  with vertices  $0, a, b, c$  where  $a, b, c$  lie in  $P^1(\mathbb{C}) = \partial\mathbb{H}^3$ .



*Proof.* If  $x$  is another point in  $P^1(\mathbb{C})$ , then it is well known [15] that

$$CD_2 r(x, a, b, c) = \text{vol}(T_{xabc}) \quad (4)$$

for some constant  $C$ . In [15] the value of  $C$  is reported to be  $3/2$  but Jun Yang has pointed out to us that the correct value of  $C$  is 1. This is because the ideal regular tetrahedron has vertices  $\infty, z, \omega z, \omega^2 z$  where  $\omega$  is a primitive third root of 1 and  $z$  is a square root of  $1/2$ . The cross-ratio is  $r(\infty, z, \omega z, \omega^2 z) = -\omega^2$  not  $\omega$  and  $D_2(-\omega^2) = 3/2 D_2(\omega)$ .

It is geometrically obvious that

$$\text{vol}(T_{xabc}) = \text{vol}(T_{0abc}) - \text{vol}(T_{0xbc}) + \text{vol}(T_{0xac}) - \text{vol}(T_{0xab}). \quad (5)$$

If we average (5) over all  $x$  in  $P^1(\mathbb{C})$  the last three terms on the right vanish. For example, the average value of  $\text{vol}(T_{0xab})$  is zero since by a unitary transformation we may assume that both  $a$  and  $b$  have real coordinates. Consequently  $\text{vol}(T_{0abc})$  is the average value of  $\text{vol}(T_{xabc})$  which is equal to  $l(a, b, c)$  by (4) and the definition of  $l(a, b, c)$ .  $\square$

## 2. The Pictures $L_n$

The rational generators for  $K_3$  of cyclotomic number fields are represented by pictures constructed from geometrically identical pieces. One of these pieces is given in Figure 2.1. This drawing is called a 'partial picture' because it has loose ends. These are the six edges leading off the top, bottom and sides of Figure 2.1. When

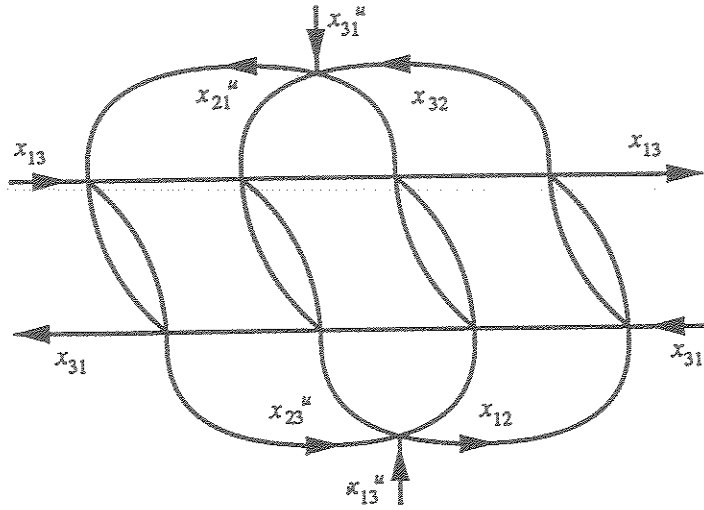


Fig. 2.1.

read counterclockwise starting at 11 o'clock, the labels on these six edges are:  $x_{13}^1, x_{31}^{-1}, x_{13}^u, x_{31}^1, x_{13}^{-1}, x_{31}^u$ . (We invert the labels on the outward oriented edges.) The product of these six elementary operations is trivial in the Steinberg group  $\text{St}(R)$  of any ring  $R$  for any  $u \in R$ . Figure 2.1 is a geometric representation of the following proof of this relation.

$$\begin{aligned}
 & x_{13}^1 x_{31}^{-1} x_{13}^u x_{31}^1 x_{13}^{-1} x_{31}^u \\
 &= x_{13}^1 x_{31}^{-1} [x_{12}^1, x_{23}^u] x_{31}^1 x_{13}^{-1} x_{31}^u \\
 &= x_{13}^1 [x_{31}^{-1} x_{12}^1 x_{31}^1, x_{31}^{-1}, x_{23}^u x_{31}^1] x_{13}^{-1} x_{31}^u \\
 &= x_{13}^1 [x_{12}^1 x_{32}^{-1}, x_{21}^u x_{23}^u] x_{13}^{-1} x_{31}^u \\
 &= [x_{32}^{-1}, x_{21}^u] x_{31}^u \\
 &= 1.
 \end{aligned} \tag{0}$$

Now suppose that  $u$  is a unit in  $R$  and let  $D$  be any element of  $\text{St}(R)$  representing the diagonal matrix  $\text{diag}(1, 1, u, u^{-1})$ , e.g.  $D = h_{34}(u)$ . Then we note that

$$x_{13}^{-1} x_{31}^u = D x_{13}^{-1} x_{31}^1 D^{-1} = D (x_{13}^{-1} x_{31}^1)^{-1} D^{-1}.$$

If we write  $w = x_{13}^{-1} x_{31}^u$ , then the relation in (0) becomes  $x_{13}^1 w x_{31}^1 x_{31}^u (D w D^{-1})^{-1}$ . If we now assume that  $u$  satisfies the relation  $1 + u + u^2 + \cdots + u^{n-1} = 0$  (and consequently  $u^n = 1$ ) then we can form a complete picture with no loose ends as indicated schematically in Figure 2.2. The square labelled  $Q$  represents Figure 2.1 and  $D^k Q D^k$  represents Figure 2.1 with the edge labels conjugated by  $D^k$ .

Figure 2.3 is an example of Figure 2.2 in the case  $n = 2$ . For aesthetic reasons, we have moved half of the  $w = D^n w D^{-n}$  double line in Figure 2.2 to the top of Figure 2.3 so that the two points  $a, b$  in Figure 2.3 represent the two vertices in Figure 2.2.

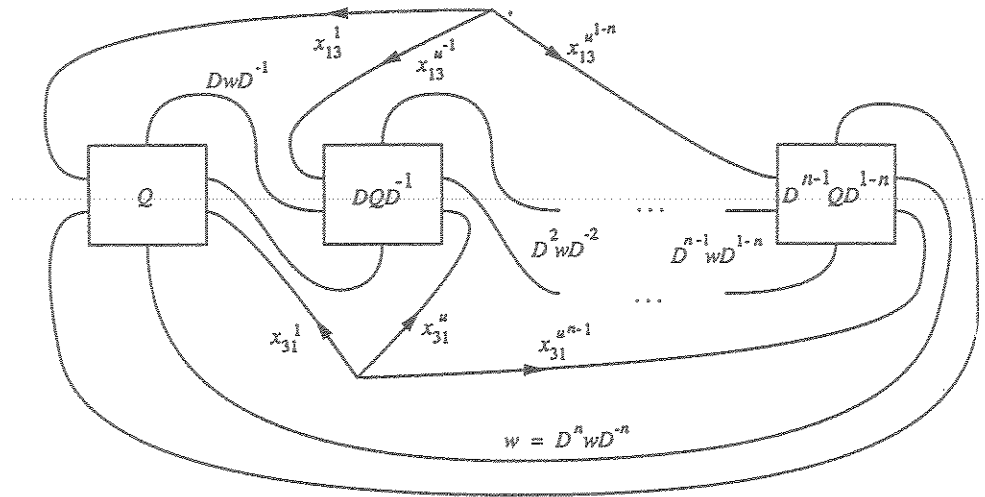


Fig. 2.2.

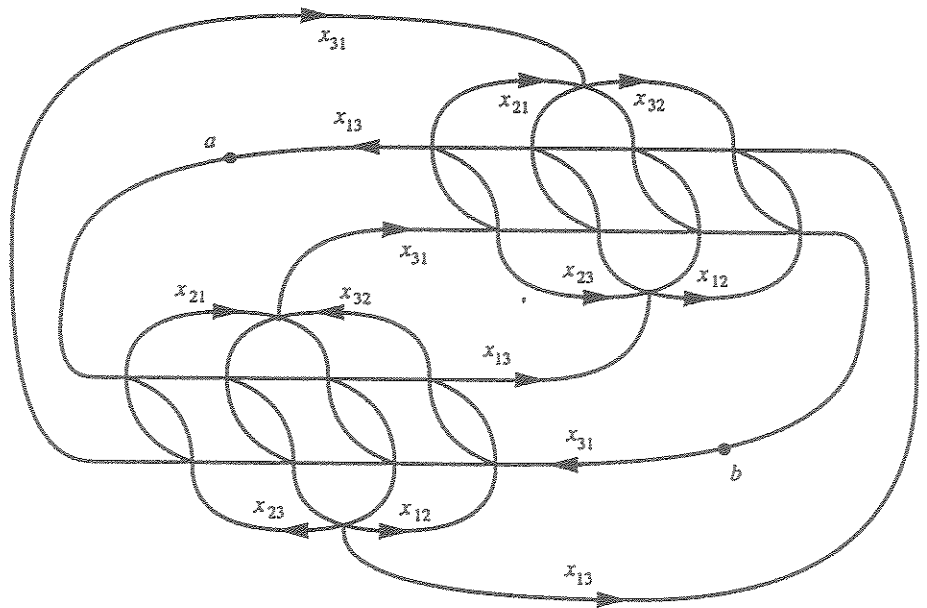


Fig. 2.3.

Also we deleted the superscripts in  $x_{ij}^1$  when they are 1. Figure 2.2 represents an element of  $K_3 Z_n$  where  $Z_n = \mathbb{Z}[u]/(1 + u + \cdots + u^{n-1})$ . We will call this element  $L_n$  since it comes from the lens space  $L(n; 1, 1)$ .

For any  $n$ th root of unity  $\xi \neq 1$  let  $\mathbb{Z}[\xi]$  denote the ring of integers in  $\mathbb{Q}(\xi)$  and let  $f_\xi: Z_n \rightarrow \mathbb{Z}[\xi]$  be the ring map which sends  $u$  to  $\xi$ .

THEOREM 2.4. *The value of the Borel regulator map on  $f_\xi(L_n)$  is the imaginary part of*

$$n \operatorname{dilog}(\xi) = n \sum_{k=1}^{\infty} \frac{\xi^k}{k^2}.$$

*Remarks 2.5.* (a) Bloch was the first to give an explicit construction of the rationally nontrivial elements of  $K_3\mathbb{Z}[\xi]$ . In fact, Bloch's elements seem to be more or less the same as ours (see [1], [16]). Beilinson [2] constructed rational elements of  $K_{2k-1}\mathbb{Z}[\xi]$  using Loday symbols and outlined a proof that the value of the regulator on these elements is  $L_k(\xi)$ . This is  $\operatorname{im} \operatorname{dilog}(\xi)$  in the case  $k = 2$ . A complete proof is given in [14] and [4].

(b) Using the formula for the Stiefel–Whitney invariant  $w_2: K_3\mathbb{Z} \rightarrow \mathbb{Z}/2$  given in Theorem 7.7 of Part I it is fairly easy to check that  $L_2$  (Figure 2.3) represents one of the exotic elements of  $K_3\mathbb{Z}$ , i.e.,  $L_2$  does not lie in the well-understood index 2 subgroup  $\mathbb{Z}/24$  of  $K_3\mathbb{Z} = \mathbb{Z}/48$  [13]. In fact,  $L_2$  can be deformed into Figure 7.6 of Part I and therefore represents a generator of  $K_3\mathbb{Z}$ . Also according to a transfer formula to be explained in a future paper  $f_\xi(L_n)$  maps to an exotic element of  $K_3\mathbb{Z}$  under the transfer map  $K_3\mathbb{Z}[\xi] \rightarrow K_3\mathbb{Z}$  if and only if  $n$  is a power of 2. (We checked this by direct computation when  $n = 4$ .) This implies that  $f_\xi(L_n)$  is not divisible by 2 when  $n$  is a power of 2.

*Proof.* The picture for  $f_\xi(L_n)$  is the same as  $L_n$  except that each  $u$  is replaced by  $\xi$ . Thus it suffices to show that the regulator map on  $L_n$  is  $n \operatorname{im} \operatorname{dilog}(u)$  when  $u$  is a unit complex number  $\neq 1$ .

The first step is to determine the matrix labels for the various regions in  $L_n$ . These are uniquely determined by the matrix  $A$  on the unique unbounded region of  $L_n$ . We usually take  $A$  to be the identity matrix but here we will take it to be

$$A = \begin{pmatrix} 1-u & 0 & -u \\ 0 & 1 & 0 \\ 0 & 0 & 1 \end{pmatrix}.$$

The choice of the invertible matrix  $A$  does not change the value of the regulator on  $L_n$ . The reason is that  $A$  is the product of a nonsingular diagonal matrix  $B$  and an upper triangular matrix  $T$ . Thus, by introducing circles of elementary operations surrounding  $L_n$  we can assume that the matrix on the region inside the added circles and outside  $L_n$  is equal to  $A \oplus B^{-1}$ . Since the formula for the regulator uses only the projectivized columns of the matrices in each region this is the same as labeling this intermediate region with the matrix  $A \oplus I$ .

Our choice of the matrix  $A$  (given by Morse theory in Part B) has the property that  $AE_{13}(-1) = DAD^{-1}$ . Consequently, the value of the regulator on each of the  $n$  pieces of  $L_n$  becomes identical and it suffices to show that  $q_\sigma(Q) = \operatorname{im} \operatorname{dilog}(u)$

for the matrix labeling of the regions in  $Q$  given in Figure 2.6 for any ordering  $\sigma$  of  $\{1, 2, 3\}$ .

If we take  $\sigma$  to be the standard ordering  $1 < 2 < 3$ , then we get exactly five nonzero terms at the corners indicated in Figure 2.6. The other corners give zero for one of three reasons. First, if either of the two edges forming a corner is labelled  $x_{ij}^r$ , where  $i < j$ , then it contributes nothing. Second, if the two edges are labelled  $x_{ik}^r, x_{jk}^s$  for the same  $k$  then it gives zero. The remaining cases are when the edges are labelled  $x_{32}^r$  and  $x_{i1}^s$  where  $i = 2$  or  $3$ . In that case the corner contributes  $\pm pS(a, b, c) = \pm p(\overline{ab}, \overline{bc}, \overline{ca})$ , where  $a, b, c$  denote the columns of the matrix label in the corner region and the sign  $+/-$  depends on whether  $x_{32}^r$  is on the clockwise/counterclockwise side of the corner.

Most of the remaining corners give zero by Corollary 1.5 which says that  $pS(x, y, z) = 0$  if two of the projective lines  $\overline{xy}, \overline{yz}, \overline{zx}$  are orthogonal. The five nonzero terms in  $q_\sigma(Q)$  are

$$\begin{aligned} pS \begin{pmatrix} 1-u & 0 & -u \\ -u & 1 & -u \\ 0 & 0 & 1 \end{pmatrix} &= pS \begin{pmatrix} 1-u & 0 & -u \\ -u & 1 & -u \\ 0 & 0 & u \end{pmatrix} \\ &= pS \begin{pmatrix} 1-u & 0 & 1 \\ -u & 1 & 1 \\ 0 & 0 & -1 \end{pmatrix} = pS(z, x, y), \end{aligned} \quad (1)$$

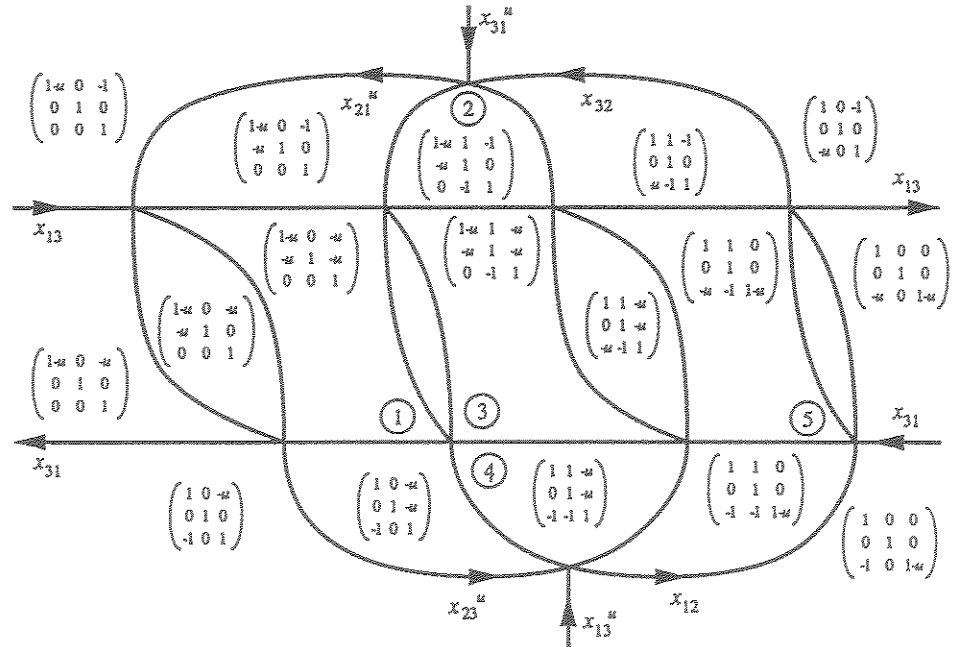


Fig. 2.6.

$$-pS(z, y, d) = pS(y, z, d), \quad (3)$$

$$pS(b, \gamma, d), \quad (4)$$

$$pS \begin{pmatrix} 1 & 1 & 0 \\ 0 & 1 & 0 \\ -u & -1 & 1-u \end{pmatrix} = pS \begin{pmatrix} 1 & 1 & 0 \\ 0 & 1 & 0 \\ -u & -1 & 1 \end{pmatrix} = pS(a, y, e), \quad (5)$$

where

$$x = (0, 1, 0)^t, \quad y = \begin{pmatrix} \frac{1}{\sqrt{2}} \\ \frac{1}{\sqrt{2}} \\ 0 \end{pmatrix}, \quad z = \begin{pmatrix} \frac{1}{\sqrt{2}} \\ -\frac{1}{\sqrt{2}} \\ 0 \end{pmatrix}.$$

$$a = (1, 0, -u)^t, \quad b = (-1, 0, 1)^t, \quad c = (1, 0, 0)^t,$$

$$d = (-u, -u, 1)', \quad e = (0, 0, 1)'$$

(see Figure 2.7). In the cases (1), (5), we made simplifications by left unitary transformations and diagonal right transformations.

The sum of these five terms can be computed as follows. By Proposition 1.7 in Part IB, the sum of the terms (2), (3), (4) gives

$$pS(y, b, z) + pS(y, z, d) + pS(y, d, b) = l(d, b, z) - l(\overline{yd}, \overline{yb}, \overline{yz}). \quad (6)$$

The same formula applied to (5) gives

$$pS(a, y, e) = l(a, b, e) - l(\overline{ya}, \overline{yb}, \overline{ye}). \quad (7)$$

(Since  $\overline{yb}$  is perpendicular to  $\overline{ab} = \overline{be}$ , the terms  $pS(y, a, b)$  and  $pS(y, b, e)$  vanish by Corollary 1.5). Since  $\overline{ya} = \overline{yz}$  and  $\overline{ye} = \overline{yd}$  the sum of (6) and (7) is  $l(a, b, e) + l(d, b, z)$ . Finally by Theorem 1.4 we get

$$pS(x, y, z) = l(a, y, z) - l(a, b, c).$$

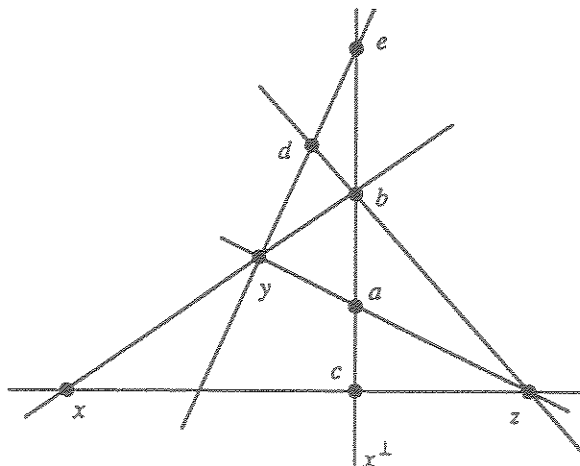


Fig. 2.7.

However, the unitary matrix  $\text{diag}(u, u, 1)$  transforms  $(a, y, z)$  to  $(b, d, z)$  and, therefore,  $l(a, y, z) = l(b, d, z)$ . The sum of our five terms is therefore equal to

$$q_\sigma(Q) = l(a, b, e) - l(a, b, c) = D_2 r(a, b, c, e) = D_2 r(u, 1, \infty, 0) = D_2(u),$$

since  $c \perp e$ . □

## PART B: MORSE THEORY ON CIRCLE BUNDLES

In this part of the paper we will indicate how the pictures  $(L_n)$  in Part A were obtained from circle bundles over  $S^2$ . Since we are extracting an intricate algebraic invariant out of something which is geometrically very elementary, this is not a good example of the use of algebraic invariants in topology. However, we are hopeful that this analysis will lead to a better understanding of those fiber homotopically trivial but smoothly non-trivial bundles over  $S^2$  which are detected by the same invariant. (See Theorem 7.1 below.)

### 1. The Space of Positively Oriented GMF's on $S^1$

It is easy to see that the space of Morse functions on the circle  $S^1$  is homotopy equivalent to a disjoint union of infinitely many circles. However, if we allow cubic singularities we get a connected space of functions and if we allow only 'positive' cubic singularities we get a contractible space of functions. With the definitions below this is equivalent to saying that any oriented  $S^1$  bundle admits a fiberwise 'positively oriented generalized Morse function' which is unique up to homotopy.

**DEFINITION 1.1.** A smooth function  $f: S^1 \rightarrow \mathbb{R}$  is called a *generalized Morse function* (GMF) if for every  $x \in S^1$  one of the first three derivatives of  $f$  at  $x$  is nonzero. We say that  $f$  is a *positively oriented GMF* (PGMF) if  $f'''(x) > 0$  whenever  $f'(x) = f''(x) = 0$ .

Let  $\text{PGMF}(S^1)$  denote the space of all PGMF's on  $S^1$  with the  $C^\infty$  topology. The following drawing (Figure 1.2) illustrates a family of PGMF's on  $S^1$ . The function  $f$  is the height function (the distance from the bottom of the page).

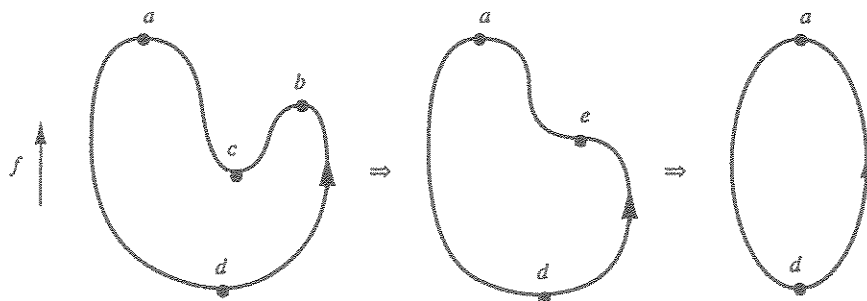


Fig. 1.2.

We see in Figure 1.2 that a relative maximum  $b$  can be cancelled with a relative minimum  $c$  by a deformation of PGMF's on  $S^1$  (i.e. a path in  $\text{PGMF}(S^1)$ ) provided that the local minimum  $c$  is directly counterclockwise from  $b$  and there is at least one other local minimum (d).

We will show that the space  $\text{PGMF}(S^1)$  is contractible. The proof is based on the following simple observations.

LEMMA 1.3. *For any  $f \in \text{PGMF}(S^1)$  let  $F(f)$  be the space of all  $g \in \text{PGMF}(S^1)$  so that  $f, g$  have the same local maxima, minima and cubic points. Then  $F(f)$  is convex and thus contractible.*  $\square$

This lemma tells us that a PGMF on  $S^1$  is uniquely determined up to 'contractible choice' by its configuration of critical points, i.e. the set of critical points together with the data of which are local minima, maxima and cubic points. If  $x_1 < x_2 < \dots < x_n$  are the critical points of  $f$  in cyclic order which are not local minima then  $n \geq 1$  and the critical points  $y_i$  of  $f$  which are not local maxima can be numbered so that

$$x_1 \leq y_1 < x_2 \leq y_2 < \dots < x_n \leq y_n < x_1 + 2\pi \quad (1)$$

in cyclic order (and  $x_i \neq y_i$  for at least one  $i$ ). Consequently, the  $x_i$ 's determine the  $y_i$ 's up to contractible choice.

As the function  $f$  varies the set of  $x$ 's moves continuously and sometimes elements appear and disappear. This means we are talking about the 'topological poset' of all finite nonempty subsets of  $S^1$  ordered by inclusion. This poset  $P$  is obviously contractible since it has a cofinality property, namely given any finite collection of elements  $A_i$  of  $P$  there is another  $B$  in  $P$  disjoint from each  $A_i$  and thus  $A_i \subseteq B \cup A_i \supseteq B$ .

It is not difficult to make this argument rigorous. We begin at the end with the poset  $P$ .

Let  $P$  be the space of all finite nonempty subsets of  $S^1$  topologized in the obvious way so that it is a disjoint union of manifolds without boundary each homotopy equivalent to  $S^1$ . The nerve of  $P$  is the simplicial space  $N_\bullet P$  which in degree  $k$  is given by all sequences of elements  $A_0 \leq A_1 \leq \dots \leq A_k$  of  $P$  (ordered by inclusion) and topologized as a subspace of  $P^{k+1}$ . For each  $k \geq 0$  we note that  $N_k P$  is the disjoint union  $N_k^{\text{deg}} P \amalg N_k^{\text{nd}} P$  where  $N_k^{\text{nd}} P$  is the space of all sequences  $A_0 < A_1 < \dots < A_k$  in  $P$ . This implies that the geometric realization  $|N_\bullet P|$  of  $N_\bullet P$  is naturally homeomorphic to the nondegenerate realization of  $N_\bullet^{\text{nd}} P$  given by

$$\|N_\bullet^{\text{nd}} P\| = \amalg \Delta^k \times N_k^{\text{nd}} P / \sim$$

where only face maps are used in the identifications.

LEMMA 1.4. *The geometric realization  $|P| = |N_\bullet P| \cong \|N_\bullet^{\text{nd}} P\|$  of  $P$  is contractible.*

*Proof.* If  $A \in P$  let  $P_A$  be the space of all  $B$  in  $P$  which are disjoint from  $A$ . Then the elements of any compact subset  $K$  of  $P_A$  are disjoint from a neighborhood  $U_K$  of

$A$  in  $S^1$ . In particular, there is an  $x \in S^1 \setminus A$  so that  $x$  is disjoint from each  $B \in K$ . The inclusions  $B \subseteq B \cup \{x\} \supseteq \{x\}$  give a null homotopy of the inclusion map  $|N, K| \rightarrow |N, P_A|$ . Since any compact subset of  $|N, P_A|$  is contained in  $|N, K|$  for some compact  $K \subseteq P_A$  this proves that  $|P_A| = |N, P_A|$  is contractible.

On the other hand  $\cap |P_{A_i}| = |P_{\cup A_i}|$  so any finite intersection of  $|P_{A_i}|$ 's is contractible. By induction on  $n$  it follows that any union of  $n \geq 1$   $|P_{A_i}|$ 's is also contractible. Since the  $|P_{A_i}|$ 's form an open covering of  $|P|$  any compact subset of  $|P|$  is contained in a union of finitely many  $|P_{A_i}|$ 's. Since  $|P|$  has the homotopy type of a CW complex we conclude that it is contractible.  $\square$

For each  $n \geq 1$  let  $Q_n$  be the space of all ordered pairs  $(X, Y)$  where  $X, Y$  are subsets of  $S^1$  of size  $n$  satisfying the condition that the inequality (1) holds for some ordering of the elements of  $X, Y$  and so that  $X \neq Y$ . Let  $Q = \coprod Q_n$  with partial ordering given by  $(X, Y) \leq (X', Y')$  if  $X \subseteq X', Y \subseteq Y'$  and  $X' \setminus X = Y' \setminus Y$ . As in the case of the topological poset  $P$ ,  $|Q| = |N, Q|$  is homeomorphic to  $\|N^{nd}Q\|$ .

LEMMA 1.5. *The geometric realization of  $Q$  is contractible.*

*Proof.* The projection to the first coordinate gives an order preserving continuous map  $p: Q \rightarrow P$  and consequently a nondegenerate simplicial map  $N^{nd}_* p: N^{nd}_* Q \rightarrow N^{nd}_* P$ . For each  $k \geq 0$ ,  $N^{nd}_k p: N^{nd}_k Q \rightarrow N^{nd}_k P$  is a homotopy equivalence and so  $|Q| \cong \|N^{nd}_* Q\| \simeq \|N^{nd}_* P\| \cong |P| \simeq *$ .  $\square$

Now we need an explicit description of the elements of the geometric realization of  $Q$ . For each  $n \geq 1$  let  $M_n$  be the space of all triples  $(X, Y, f)$  where  $(X, Y) \in Q_n$  and  $f: X \cup Y \rightarrow [0, 1]$  is a function satisfying the property that  $f$  sends the complement of  $X \cap Y$  to 1. We use the notation  $X_+, Y_+$  to denote  $X \setminus f^{-1}(0), Y \setminus f^{-1}(0)$ , respectively.

Let  $M$  be the quotient space of  $\coprod M_n$  given by the identification  $(X, Y, f) \sim (X', Y', f')$  if  $X_+ = X'_+, Y_+ = Y'_+$  and  $f|_{X_+ \cup Y_+} = f'|_{X'_+ \cup Y'_+}$ .

LEMMA 1.6.  *$M$  is homeomorphic to  $|Q|$  and thus contractible.*

*Proof.* We will construct continuous inverse maps  $|F|: |Q| \rightarrow M$  and  $G: M \rightarrow |Q|$ . For each  $k \geq 0$  let  $F_k: \Delta^k \times N^{nd}_k Q \rightarrow M$  be given by

$$F_k(t, (X_0, Y_0) < \cdots < (X_k, Y_k)) = (X_k, Y_k, f_t),$$

where  $f_t: X_k \cup Y_k \rightarrow [0, 1]$  is given by  $f_t(z) = \sum t_i$  where the sum is taken over all  $i$  s.t.  $z \in X_i \cup Y_i$  (in particular  $f_t(z) = 1$  if  $z \in X_0 \cup Y_0$ ). One can check that the maps  $F_k$  are compatible with face operators and thus define a continuous map  $|F|: \|N^{nd}_* Q\| \rightarrow M$ .

For each  $k \geq 0$  let  $M^k$  be the subspace of  $M$  consisting of all  $(X, Y, f)$  where  $f: X \cup Y \rightarrow [0, 1]$  takes exactly  $k$  values  $v_1 > v_2 > \cdots > v_k$  in the open interval  $(0, 1)$ . Note that  $M^0 \cup \cdots \cup M^k$  is a closed subset of  $M$  for all  $k$ . Let  $G_k: M^k \rightarrow \Delta \times N^{nd}_k Q$  be given by

$$G_k(X, Y, f) = (t, (X_0, Y_0) < \cdots < (X_k, Y_k))$$

where

$$t_i = v_i - v_{i+1} \quad (v_0 = 1, v_{k+1} = 0), \quad X_i = X \cap f^{-1}[v_i, 1] \quad \text{and} \\ Y_i = Y \cap f^{-1}[v_i, 1].$$

Then  $G = \bigcup G_k: M \rightarrow |Q|$  defines a set-theoretic inverse for  $|F|$  and, thus,  $|F|$  is a continuous bijection. If a sequence of elements  $A_i$  of  $M^k \cap M_n$  converges to an element  $B$  of  $M^m \cap M_n$ , where  $m < k$  then  $t$  converges to the boundary of  $\Delta^k$  and  $G_k(A_i)$  converges to  $G_m(B)$ . Since  $M_n$  is locally compact, this means that  $G$  is continuous and, hence, a homeomorphism  $M \cong |Q|$ .  $\square$

**THEOREM 1.7.**  $\text{PGMF}(S^1)$  is contractible.

*Proof.* Let  $\mathcal{F}$  be the space of all smooth maps  $f: S^1 \rightarrow \mathbb{R}$  with the following properties.

- (a) For each  $x \in f^{-1}(0)$  either  $f'(x) \neq 0$  or  $f''(x) > 0$ .
- (b) There is at least one  $x \in S^1$  so that  $f(x) = 0$  and  $f'(x) \neq 0$ .

We claim that  $\text{PGMF}(S^1) \simeq \mathcal{F} \simeq M \cong |Q|$ .

By integration and differentiation it is evident that  $\text{PGMF}(S^1)$  is homeomorphic to  $\mathbb{R} \times \mathcal{F}_0$ , where  $\mathcal{F}_0$  is the subspace of  $\mathcal{F}$  given by the condition

$$\int_0^{2\pi} f(x) dx = 0. \quad (2)$$

But a deformation retraction of  $\mathcal{F}$  to  $\mathcal{F}_0$  is given by  $H(f, t)(x) = e^{ctf(x)}f(x)$  where  $c = c(f)$  is given implicitly by

$$\int_0^{2\pi} e^{cf(x)}f(x) dx = 0. \quad (3)$$

Note that the derivative of (3) with respect to  $c$  is bounded below by

$$\min \left( \int_0^{2\pi} \max(0, f(x))^2 dx, \int_0^{2\pi} \min(0, f(x))^2 dx \right).$$

Thus (3) determines  $c$  uniquely and  $c(f)$  is a continuous function of  $f$  by the implicit function theorem. This proves that  $\text{PGMF}(S^1) \simeq \mathcal{F}$ .

We will now construct continuous maps  $\alpha: \mathcal{F} \rightarrow M$  and  $\beta: M \rightarrow \mathcal{F}$  so that the composition  $\beta\alpha$  is homotopic to the identity on  $\mathcal{F}$ . Since  $M$  is contractible  $\beta\alpha$  must also be null homotopic.

For each  $f \in \mathcal{F}$  let  $\delta(f)$  be the minimum distance from the 3-jet  $(f(x), f'(x), f''(x))$  of  $f$  to the subset  $J = 0 \times 0 \times (-\infty, 0]$  of  $\mathbb{R}^3$ . Then  $\delta(f) > 0$  and  $\delta: \mathcal{F} \rightarrow M$  is

continuous. Let  $\alpha: \mathcal{F} \rightarrow M$  be given by  $\alpha(f) = (X, Y, h)$  where

$$Z = X \cap Y = \{z \in S^1 \mid f'(z) = 0 \text{ and } 0 \leq f(z) < \delta(f)\},$$

$$X = Z \cup \{x \in S^1 \mid f(x) = 0, f'(x) < 0\},$$

$$Y = Z \cup \{y \in S^1 \mid f(y) = 0, f'(y) > 0\},$$

$$h(z) = 1 - f(z)/\delta(f) \text{ for all } z \in X \cup Y.$$

Let  $\beta: M \rightarrow \mathcal{F}$  be given by

$$\begin{aligned} \beta(X, Y, h)(t) &= \prod_{x_i \in X \setminus Z} \sin \tfrac{1}{2}(x_i - t) \prod_{y_i \in Y \setminus Z} \sin \tfrac{1}{2}(y_i - t) \prod_{z \in Z} (1 - h(z) + h(z) \sin^2 \tfrac{1}{2}(z - t)), \end{aligned}$$

where  $Z = X \cap Y$  and  $x_i, y_i \in \mathbb{R}$  are chosen to satisfy (1). Since  $\beta\alpha(f)$  has the same configuration of critical points as  $f$ , it follows from Lemma 1.3 that  $\beta\alpha$  is homotopic to the identity on  $\mathcal{F}$ . Since  $M$  is contractible, we conclude that  $\mathcal{F}$  is contractible.  $\square$

## 2. Fiberwise PGMF's on $S^1 \times S^1$

The proof of Theorem 1.7 (the contractibility of  $\text{PGMF}(S^1)$ ) gives a procedure for constructing a fiberwise PGMF on any smooth oriented circle bundle. This procedure will be explained for the trivial bundle  $S^1 \times S^1 \rightarrow S^1$  in this section and will be applied to nontrivial  $S^1$ -bundles over  $S^2$  in Section 5. Trivial bundles give trivial algebraic invariants so we will get only trivial elements of  $K_2 R$  in this section. However, the discussion will make the next case easier.

Let  $p: E^{n+1} \rightarrow B^n$  be a smooth oriented  $S^1$ -bundle where  $B$  is a closed  $n$ -manifold. Then we would like to construct a fiberwise PGMF for  $E$ , i.e. a smooth map  $f: E \rightarrow \mathbb{R}$  so that  $f$  is a PGMF on each fiber of  $p$ . The first step in the construction of such a map is to find a system of smoothly embedded  $n$ -disks  $D_1, \dots, D_m$  in  $E$  so that  $p: D_i \rightarrow B$  is an embedding for all  $i$  and the interiors of the  $D_i$ 's cover  $B$ . Two examples are given in Figure 2.1 for the bundle  $p: S^1 \times S^1 \rightarrow S^1$ . The existence and 'uniqueness' of the disks  $D_i$  will be proved at the end of the section. It is more or less equivalent to the contractibility of  $|P|$  (Lemma 1.4) since the disks determine a section of the  $|P|$ -bundle associated to  $E$ .

The second step in the construction of  $f: E \rightarrow \mathbb{R}$  is to expand the disks  $D_i$  into configurations of singularities. The boundary points of each  $D_i$  should become the cubic singularities and the interior points of each disk should be replaced by max-min pairs as indicated in Figure 2.2. Note that each  $n$ -disk  $D_i$  is replaced by an  $n$ -sphere  $S_i$  whose image in  $B$  is the same as the image of  $D_i$ . In Figure 2.2 the (formal) local maxima are indicated by the solid lines and the (formal) local minima

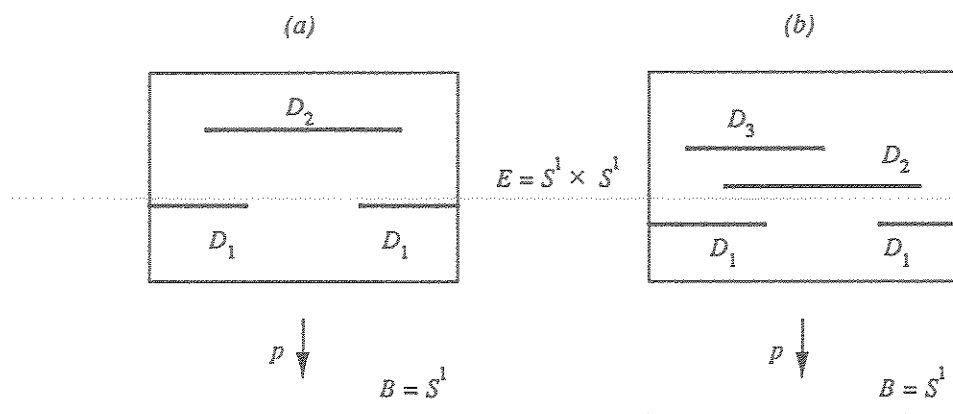


Fig. 2.1.

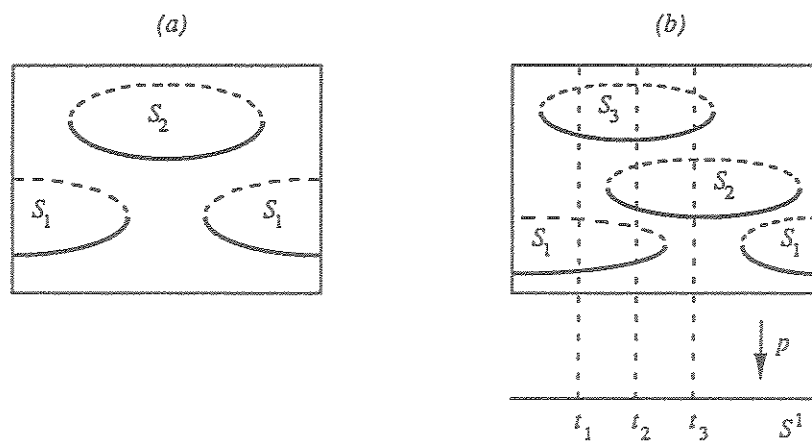


Fig. 2.2.

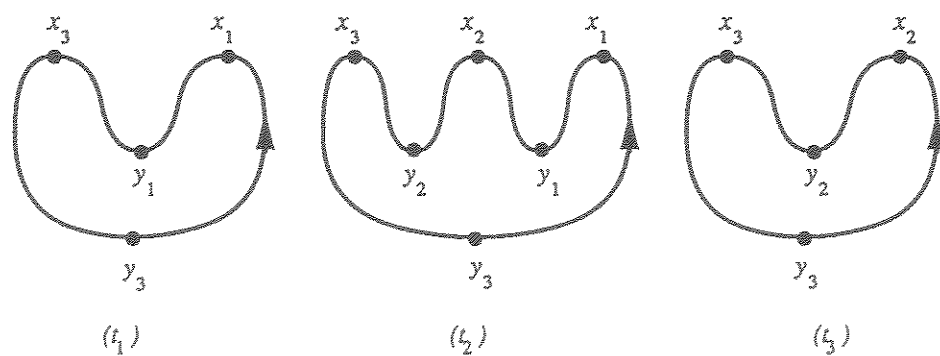


Fig. 2.3.

by dotted lines. The diagrams in Figure 2.2 give sections of the  $|Q|$ -bundle associated to  $E$ .

Using the homotopy equivalence  $|Q| \simeq FF \simeq \text{PGMF}(S^1)$  we can construct fiberwise PGMF's  $f: E \rightarrow \mathbb{R}$  with the fiberwise critical sets given in Figure 2.2. For example over the points  $t_1, t_2, t_3$  in  $B = S^1$  the functions for 2.2(b) are indicated in Figure 2.3. The arrows in Figure 2.3 indicate the orientations of the circles and the positions of the base points.

The three Morse functions indicated in Figure 2.3 give three cell decompositions of  $S^1$ . The corresponding cellular chain complexes with twisted coefficients in a commutative ring  $R$  are given by

$$\begin{array}{ccc} R^2 & R^3 & R^2 \\ \downarrow \begin{pmatrix} 1 & -1 \\ -u & 1 \end{pmatrix} & \downarrow \begin{pmatrix} 1 & -1 & 0 \\ 0 & 1 & -1 \\ -u & 0 & 1 \end{pmatrix} & \downarrow \begin{pmatrix} 1 & -1 \\ -u & 1 \end{pmatrix} \\ R^2 & R^3 & R^2 \\ (t_1) & (t_2) & (t_3) \end{array}$$

where  $u \in R^\times$  is the inverse of the holonomy of the coefficient system over  $S^1$ . For example in  $t_2$ ,  $\partial x_1 = y_1 - uy_3$  since we must cross the base point of  $S^1$  in the reverse (clockwise) direction to get from  $x_1$  to  $y_3$ . (If  $R$  is noncommutative, we need to take right  $R$ -modules. Thus,  $\partial x_1 = y_1 - y_3u$  would be a more accurate formula.)

If we formally replace the missing critical points  $x_2, y_2$  in  $(t_1)$  and the missing points  $x_1, y_1$  in  $(t_3)$  we get the following  $3 \times 3$  matrices.

$$A_1 = \begin{pmatrix} 1 & 0 & -1 \\ 0 & 1 & 0 \\ -u & 0 & 1 \end{pmatrix}, \quad A_2 = \begin{pmatrix} 1 & -1 & 0 \\ 0 & 1 & -1 \\ -u & 0 & 1 \end{pmatrix}, \quad A_3 = \begin{pmatrix} 1 & 0 & 0 \\ 0 & 1 & -1 \\ 0 & -u & 1 \end{pmatrix}.$$

We note that each matrix is obtained from the previous matrix by one elementary row operation and one elementary column operation:

$$A_2 = E_{12}(-1)A_1E_{23}(-1), \quad (4)$$

$$A_3 = E_{31}(u)A_2E_{12}(1). \quad (5)$$

This is because the cancellation of two critical points say  $x_i, y_i$  eliminates exactly two incidences, namely the incidences of  $x_i$  over  $y_{i-1}$  and that of  $y_i$  under  $x_{i+1}$  (assuming that  $0 < x_1 < y_1 < \dots < x_m < y_m < 2\pi$ ). Thus,

$$A' = E_{i-1,i}(1)AE_{i,i+1}(1). \quad (6)$$

In the case  $i = m$ , we have

$$A' = E_{m-1,m}(1)AE_{m,1}(u), \quad (7)$$

and in the case  $i = 1$ , we have

$$A' = E_{m1}(u)AE_{12}(1), \quad (8)$$

if we take the holonomy into account. We note that (5) is a special case of (8) and (4) is a special case of (6) (with  $A' = A_1$ ,  $A = A_2$ ).

There is also a Morse theoretic explanation of (6) which will be given in the next section.

The four cubic points in Figure 2.2(a) correspond to eight elementary operations

$$y_{12}^{-1}x_{21}^{-u}x_{12}^1y_{21}^uy_{21}^{-u}x_{12}^{-1}x_{21}^uy_{12}^1, \quad (9)$$

where  $x_{ij}^r = x_{ij}(r)$  denotes the column operation  $A \mapsto AE_{ij}(r)$  and  $y_{ij}^r = y_{ij}(r)$  denotes the row operation  $A \mapsto E_{ij}(r)A$ . At a 'birth' point where a pair of critical points is created, we write the  $y$ -term first and at a 'death' or cancellation point we write the  $x$  term first. Then it is clear that the operations in (9) all cancel.

The same procedure applied to Figure 2.2(b) gives the sequence of operations

$$y_{13}^{-1}x_{31}^{-u}y_{12}^{-1}x_{23}^1x_{12}^uy_{31}^uy_{32}^1y_{23}^{-1}x_{21}^{-u}x_{12}^{-1}x_{21}^uy_{12}^1. \quad (10)$$

Since these are elementary operations which we apply to the diagonal matrix  $D = \text{diag}(1-u, 1, 1)$  to give back  $D$ , we get a matrix equation of the form  $E'_6 \dots E'_1 DE_1 \dots E_6 = D$ . Thus, the product of the elementary matrices  $(D^{-1}E'_6 D) \dots (D^{-1}E'_1 D)E_1 \dots E_6$  is the identity matrix. In other words, the formal product

$$x_{12}^{(1-u)^{-1}u}x_{21}^{-u(1-u)}x_{23}^1x_{31}^{u(1-u)}x_{21}^{-(1-u)^{-1}}x_{13}^{-(1-u)^{-1}}x_{31}^{-u}x_{23}^{-1}x_{12}^ux_{32}^1x_{12}^{-1}x_{21}^1 \quad (11)$$

gives an element of  $K_2 R$ . By the 'uniqueness' of the system of disks  $\{D_i\}$  as proved below, this is an invariant of the bundle  $S^1 \times S^1 \rightarrow S^1$  and therefore must be trivial, as in (9).

**PROPOSITION 2.4.** *Let  $B$  be a smooth closed  $n$ -manifold and let  $p: E \rightarrow B$  be a smooth bundle with positive fiber dimension. Then there exists a finite collection of disjoint smoothly embedded  $n$ -disks  $D_1, \dots, D_m$  in  $E$  so that  $p$  is an embedding on each  $D_i$  and  $\{p(\text{int } D_i)\}$  is an open covering of  $B$ . Furthermore, given another such family of disks  $\{D'_j\}$ , there exists a third family  $\{D''_k\}$  so that each  $D''_k$  is disjoint from each  $D_i$  and from each  $D'_j$ .*

*Remark.* The family of disks  $\{D''_k\}$  allows us to go 'continuously' from  $\{D_i\}$  to  $\{D'_j\}$  by first adding the new disks  $D''_k$ , eliminating the old disks, adding the disks  $D'_j$  then eliminating the disks  $D''_k$ . This creates a collection of disjoint embedded cylinders  $(D^n \times I)$  in  $E \times I$  whose interiors cover  $B \times (0, 1)$ . By rounding off those corners that lie over  $B \times (0, 1)$ , this gives a family of disjoint disks and half disks in  $E \times I$  which agree with the disks  $\{D_i\}$ ,  $\{D'_j\}$  over  $B \times 0$  and  $B \times 1$ .

*Proof.* First choose not necessarily disjoint disks  $D_i$  in  $E$  so that their interiors cover  $B$ . Then we replace each  $D_i$  by a collection of disks which are disjoint from each other and from each  $D_i$ .

Let  $m$  be maximal so that  $D_m$  is not disjoint from the other disks. Let  $U = p(\text{int } D_m)$ . Then  $p^{-1}U$  is diffeomorphic to  $U \times M$ , where  $M$  is the fiber of  $p: E \rightarrow B$ . Let  $K \subseteq U$  be the complement of the union of  $p(\text{int } D_i)$  for all  $i \neq m$ . Then  $K$  is compact. For each  $x \in K$ , there is a  $y \in M$  and a small disk neighborhood  $N(x)$  of  $x$  in  $U$  so that  $N(x) \times y$  is disjoint from all disks  $U_i$ . Choose a finite subcovering  $\{N(x_j)\}$  of  $K$ . We may assume that the corresponding elements  $y_j$  of  $M$  are distinct. By replacing the disks  $D_m$  with the disks  $N(x_j) \times y_j$ , we decrease the number  $m$ . The proof of the relative case is the same.  $\square$

### 3. The Algebra of Cubic Points I

As we saw in the last section, the incidence matrix of a PGMF on  $S^1$  changes only at cubic points. We observed in (4), (5) and more generally in (6), (7), (8), that this change in the incidence matrix can be expressed as two elementary operations. However, the same changes could also be accomplished by different sequences of elementary operations. In this section, we will do Morse theory on higher-dimensional manifolds to explain why a cubic point corresponds to exactly two elementary operations. In the next section, we will examine the algebra of PGMF's on  $S^1$  with two cubic points. Such functions occur generically in two-parameter families of PGMF's on  $S^1$  and, thus, on fiberwise PGMF's on  $S^1$ -bundles over  $S^2$ .

If  $f$  is a smooth function on a smooth manifold  $M$ , then the *positive/negative suspension* of  $f$  is defined to be the map  $\sigma_{\pm}(f): M \times \mathbb{R} \rightarrow \mathbb{R}$  given by  $\sigma_{\pm}(f)(x, y) = f(x) \pm y^2$ . The function  $f$  is *stabilized* by repeated suspension ( $s(f) = \sigma_{\pm}^n \sigma_{\mp}^m(f)$ , where  $n, m$  are both large). Since algebraic invariants such as the Whitehead torsion and Reidemeister torsion of  $\sigma_{\pm}^n \sigma_{\mp}^m(f)$  depend on the parity of  $n$ , we usually take  $n$  to be even.

If  $f \in \text{PGMF}(S^1)$  is stabilized then the local minima and maxima of  $f$  are replaced by nondegenerate critical points of  $s(f)$  of even and odd index, respectively, and the cubic points of  $f$  are replaced by birth-death points of  $s(f)$  where the function is given locally by

$$s(f)(x) = x_0^3 - \sum_{i=1}^n x_i^2 + \sum_{j=n+1}^{n+m} x_j^2 + C, \quad (12)$$

where  $C$  is a constant.

Isolated birth-death points occur generically in one-parameter families of functions and they have the important well-known property that they can be made 'independent' of all other singularities (except local maxima and minima) (see [3, 6, 9]). We recall that two critical points of a smooth function  $g$  are independent if neither is 'multiply incident' under the other where *multiple incidence* is the transitive

relation generated by 'incidence' and  $x$  is *incident* under  $y$  if there is a trajectory of the gradient of  $g$  which goes from  $x$  to  $y$ .

The purpose of making birth-death points independent from other critical points is so that the nondegenerate critical points which converge and cancel at a death point or are created at a birth point will be incident only to each other. Then at the moment of birth or death, the cellular chain complex will be changed by an elementary expansion or collapse, respectively.

The reason that birth-death points can be made independent of other critical points is that their *stable* and *unstable manifolds* are both disks. These are defined to be the subsets  $S, U$  of the level surfaces  $L_- = g^{-1}(c - \varepsilon)$  and  $L_+ = g^{-1}(c + \varepsilon)$  which are incident under and over the birth-death point respectively ( $c$  is the critical value of the birth-death point). For  $g = s(f)$  as given in (12) above, these sets are given by

$$S = \{(x, y, z) \in \mathbb{R} \times \mathbb{R}^n \times \mathbb{R}^m \mid x \leq 0, z = 0, g(x, y, z) = c - \varepsilon\},$$

$$U = \{(x, y, z) \in \mathbb{R} \times \mathbb{R}^n \times \mathbb{R}^m \mid x \geq 0, z = 0, g(x, y, z) = c + \varepsilon\}.$$

One can check that  $S$  is an  $n$ -disk and  $U$  is an  $m$ -disk. It follows that there is an isotopy of  $S$  in  $L_-$  which makes it disjoint from any closed proper subset  $K$  of  $L_-$  (assuming that  $K$  does not contain the component of  $L_-$  containing  $S$ ) or, equivalently, there is an isotopy of  $K$  in  $L_-$  moving it to a subset  $K'$  of  $L_-$  disjoint from  $S$ . If we let  $K$  be the set of all points in  $L_-$  incident over any critical point of  $g$  which is not a local minimum, then  $K$  will not contain any of the components of  $L_-$  and any isotopy of  $K$  in  $L_-$  can be accomplished either by deforming the metric as in [9] or by replacing the gradient of  $g$  by a 'gradient-like vector field' for  $g$  as in [6]. In either case  $\nabla g$  is replaced by  $\nabla' g$ . An example is given in Figure 3.1 where  $x$  is a birth-death point and  $y$  is a saddle point incident under  $x$ .

In Figure 3.1,  $S$  is a 1-disk and  $U$  is a single point. The critical point  $y$  of  $g$  is incident under the center of  $S$ . But this point can be deformed to a point  $K'$  disjoint from  $S$ . We note that during this deformation,  $K$  must cross the boundary of  $S$ .

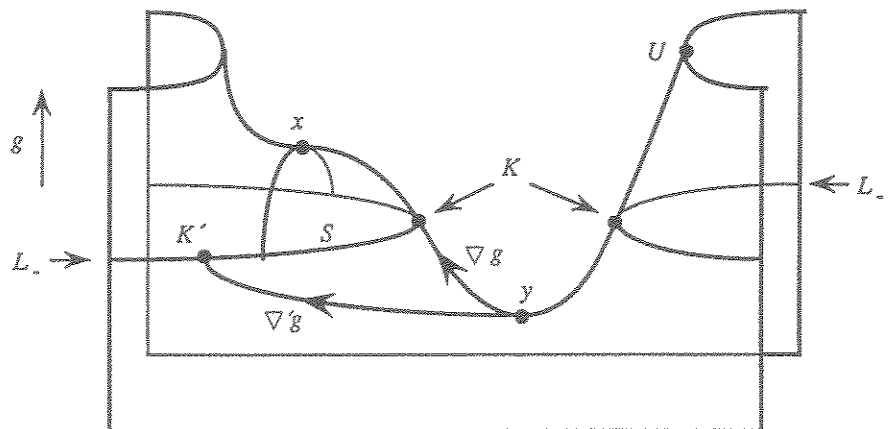


Fig. 3.1.

A higher-dimensional example is indicated in Figure 3.2 where  $L_-$  is three-dimensional,  $S$  is a 2-disk and  $K$  is a 1-sphere. The dotted line indicates the path that  $K \cap S$  follows in the isotopy. This second example is the double suspension  $(\sigma_+ \sigma_-)$  of the first example and the first example is the negative suspension of a one-dimensional example.

A birth-death point  $x$  occurring at  $t=0$  in a generic one-parameter family of functions,  $g_t$  is a point at which two nondegenerate critical points  $x_t^+$ ,  $x_t^-$  of  $g_t$  for, say,  $t > 0$  come together and cancel. This is indicated in Figure 3.3. The important feature is that the stable manifold  $S(x_t^-) \subseteq L_t$  of  $x_t^-$  is a sphere which converges to the boundary of  $S(x)$  as  $t$  goes to 0. ( $L_t$  is a level surface of  $g_t$ .) Also the set of points  $D_t$  in  $L_t$  which are incident under either  $x_t^-$  or  $x_t^+$  forms a disk with  $\partial D_t = S(x_t^-)$  so that  $D_t$  converges to  $S(x)$  as  $t \rightarrow 0$ .

If there is a saddle point  $y$  incident under  $x$  as in Figure 3.1 then it will also be incident under  $x_t^+$  (but not under  $x_t^-$ ) for  $t$  close to 0. This is indicated in Figure 3.4. (The corner set  $(\partial S(x))$  is rounded off because as  $S(x_t^-)$  converges to  $S(x)$  it is decreasing in size with infinite velocity.) For  $t$  close to 0 we need to deform  $K$  to a position  $K'$  which is disjoint from  $S(x)$ . But this necessarily creates a crossing of  $K'$  with  $S(x_t^-)$  at some value  $t_0$  of  $t$  near 0. This is an incidence between two critical

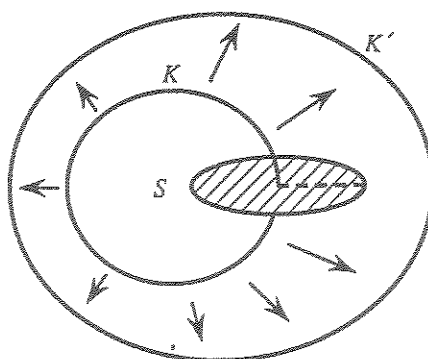


Fig. 3.2.

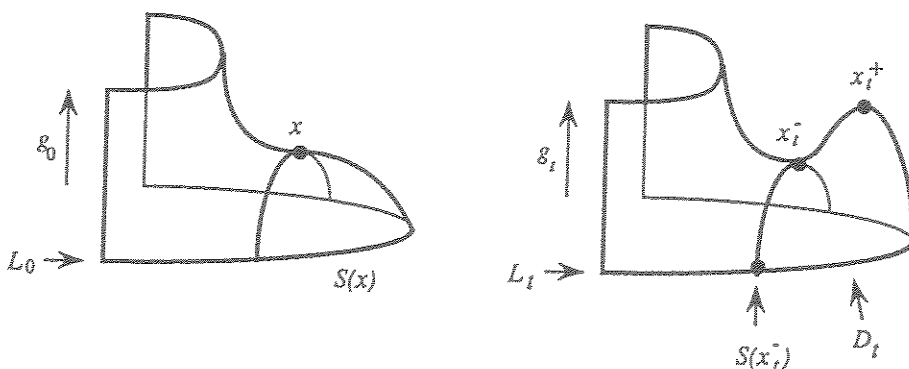


Fig. 3.3.

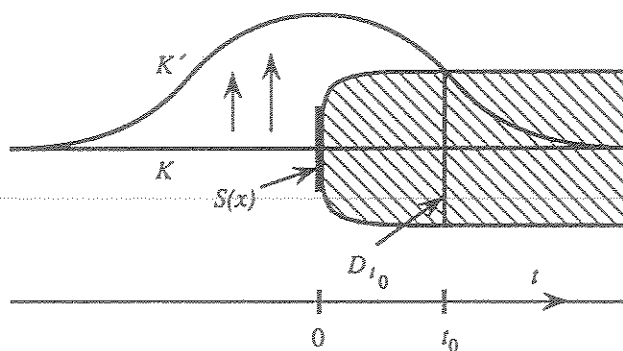


Fig. 3.4.

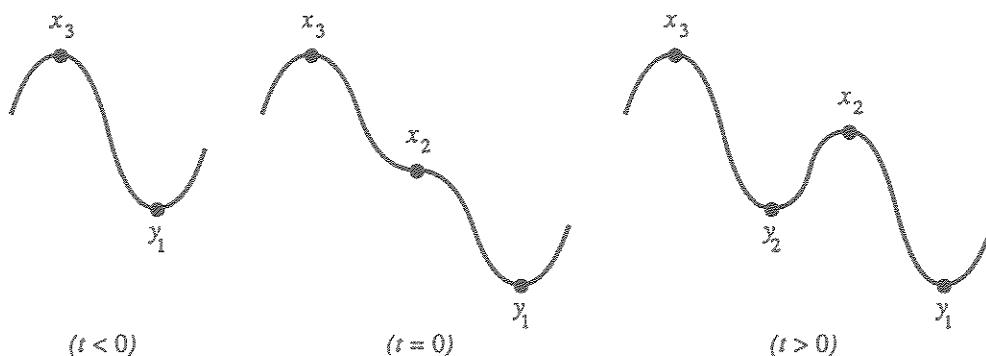


Fig. 3.5.

points  $y, x_{i_0}^-$  with the same index and therefore the incidence matrix changes by an elementary operation.

Going back to the case of PGMF's on  $S^1$ , consider the typical deformation given in Figure 3.5. After one or more negative suspensions, the incidence of  $y_1$  under  $x_2$  at  $t = 0$  can be eliminated at the expense of introducing an incidence of  $y_2$  over  $y_1$  at some  $t > 0$ . This corresponds to a row operation of the form  $y'_{12}$  for some  $r$  in the coefficient ring  $R$ . After one or more positive suspensions of  $f_t$ , the incidence of  $x_3$  over  $x_2$  at  $t = 0$  can also be eliminated but an incidence of  $x_2$  under  $x_3$  will appear at some time  $t > 0$ . This corresponds to a column operation of the form  $x'_{23}$  for some  $s$  in  $R$ . The elements  $r, s$  of  $R$  are uniquely determined by the equation

$$A' = E_{12}(r)AE_{23}(s),$$

where  $A, A'$  are incidence matrices of  $f_t$  for  $t > 0, t < 0$ , respectively. This is a special case of (6) above.

#### 4. The Algebra of Cubic Points II

We now study what happens when a PGMF on  $S^1$  has two cubic points. Such functions occur generically in two-parameter families of PGMF's on  $S^1$  which we

consider to be deformations of one-parameter families. With this interpretation the coincidence of two cubic points is actually a crossing of two cubic points as indicated in Figure 4.1.

At first glance there are three possible cases depending on whether the two cubic points are both birth points, both death points, or consist of one birth and one death point. However, these three cases are all equivalent, since they can be transformed into each other by a change of coordinates in the two-dimensional parameter space. Therefore, we consider only the case when a birth point passes a death point.

There are essentially two cases of this depending on whether the two cubic points are incident when they cross as in Figure 4.1 or they are not incident as in Figure 4.2. However, in the case of Figure 4.2, the elementary operations corresponding to the two cubic points commute. For example we get  $y_{12}^{-1}x_{23}^{-1}x_{45}^1y_{34}^1$  for 4.2(a) and  $x_{45}^1y_{34}^1y_{12}^{-1}x_{23}^{-1}$  for 4.2(b). Geometrically, the deformation in Figure 3.4 is performed for the two cubic points separately and they do not interfere with each other. Thus, we will not consider this case further.

Going back to Figure 4.1, it is very important to know the exact order of the critical values. This is shown in Figure 4.3.

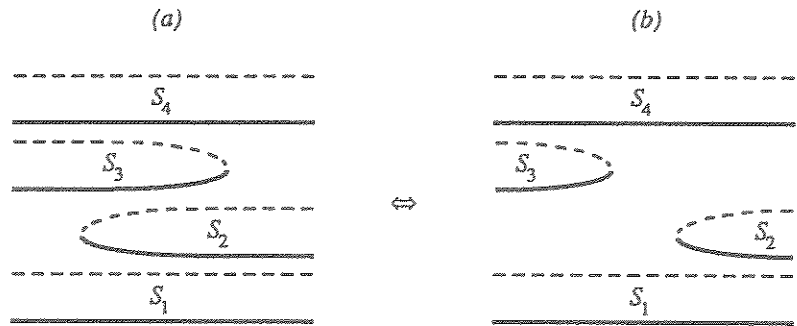


Fig. 4.1.

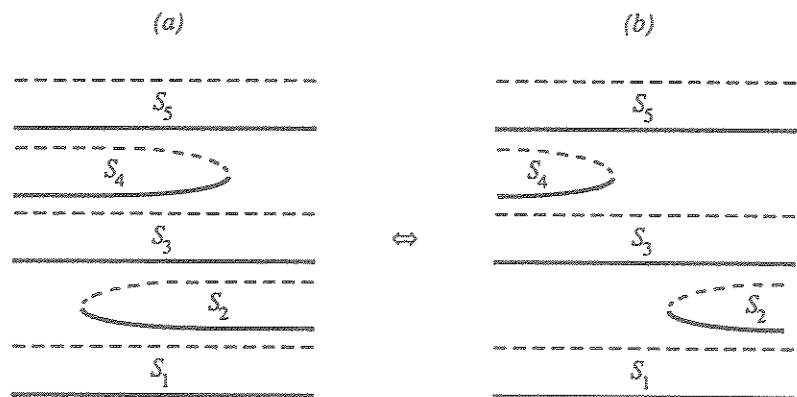


Fig. 4.2.

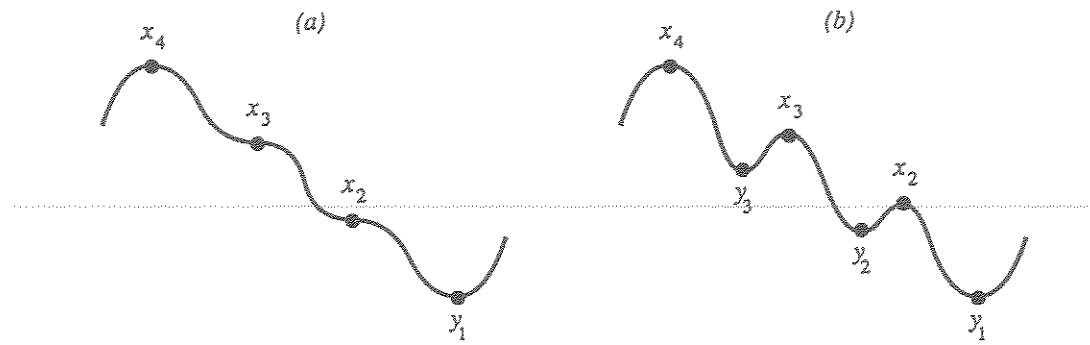


Fig. 4.3.

Evidently the ordering of the critical values is

$$f(y_1) < f(y_2) < f(x_2) < f(y_3) < f(x_3) < f(x_4). \quad (13)$$

The position of the critical values of  $x_1$  and  $y_4$  cannot be determined but they are irrelevant.

In the level surface between  $x_2$  and  $y_3$  the points incident over  $x_2$ ,  $y_2$  and those incident under  $x_3$ ,  $y_3$  are both indicated in Figure 4.4(a) for the one parameter family of functions given by Figure 4.1(a). When this family of functions is deformed to 4.1(b) these sets move to the positions shown in 4.4(c).

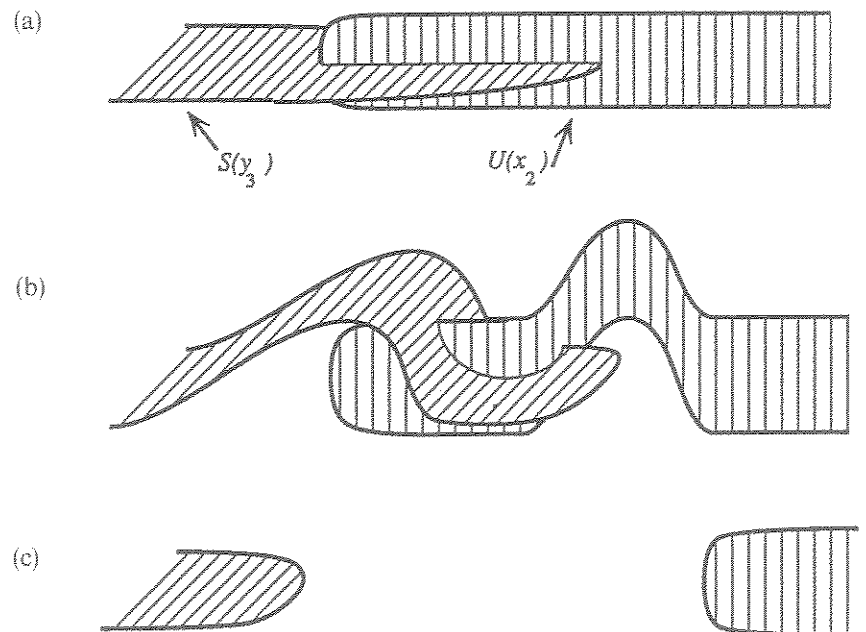


Fig. 4.4.

When the deformation 3.4 is performed on the two cubic points in 4.1(a), diagram 4.4(a) is deformed into 4.4(b). As required, the two cubic points are no longer incident to the other critical points. We must now deform 4.4(b) into 4.4(c) while maintaining the independence of the cubic points. In order to do this  $S(y_3)$  must cross  $U(x_2)$  at some point since the boundaries of the two bands are linked. In other words, there must be an incidence of  $y_3$  over  $x_2$ . Since the index of  $y_3$  is one more than the index of  $x_2$ , this is an *exchange point*. In [6], it was shown that at an exchange point the sequence of elementary operations corresponding to a one-parameter family of functions changes by an 'exchange relation' which is defined as follows.

**DEFINITION 4.5.** Let  $A$  be an  $n \times m$  matrix with coefficients in a ring  $R$  and suppose that the  $qp$ -entry of  $A$  is zero. Let  $r \in R$ . Then the *exchange relation*  $Z_{pq}^r(A)$  is the equation

$$A \Pi E_{pj}(ra_{qj}) = \Pi E_{iq}(a_{ip}r)A,$$

i.e. the sequence of elementary operations  $\Pi_j x_{pj}(ra_{qj}) \Pi_i y_{iq}(-a_{ip}r)$  is trivial on  $A$ .

For example in the case of 4.3(b), the incidence matrix is

$$A = \begin{pmatrix} 1 & -1 & 0 & 0 \\ 0 & 1 & -1 & 0 \\ 0 & 0 & 1 & -1 \\ 0 & 0 & 0 & 1 \\ \dots & & & \end{pmatrix}$$

Since  $a_{32} = 0$  we have the exchange relation  $Z_{23}^r(A)$  given by

$$AE_{23}(r)E_{24}(-r) = E_{23}(r)E_{13}(-r)A. \quad (14)$$

In other words, on the matrix  $A$  the sequence of elementary operations  $x_{23}^r x_{24}^{-1} y_{23}^r y_{13}^{-1}$  is trivial.

It was shown in [6] that (in the present notation) an exchange point where  $y_p$  is incident over  $x_q$  leads to a change in the sequence of elementary operations given by the exchange relation  $Z_{pq}^r$  where  $r$  is a unit in  $R$  determined by the geometry of the functions. (Here  $r = u$  or  $1$  depending on whether we do or do not cross the base point to go clockwise from  $y_p$  to  $x_q$  in  $S^1$ .) Indeed, we will see that the sequence of elementary operations corresponding to 4.2(a) and (b) as given in (15), (16) below differ by the exchange relation  $Z_{23}^1$ .

$$y_{12}^{-1} x_{23}^{-1} x_{34}^1 y_{23}^1, \quad (15)$$

$$x_{34}^1 y_{13}^1 y_{12}^{-1} x_{24}^{-1}. \quad (16)$$

If we let  $A$  be the matrix given above and  $B, C, D$  the matrices given by

$$B = E_{12}(1)AE_{23}(1), \quad C = E_{23}(1)AE_{34}(1),$$

$$D = E_{13}(1)BE_{34}(1) = E_{13}(1)CE_{24}(1),$$

then (15), (16) indicate two sequences of elementary operations that convert  $B$  into  $C$  and the matrices  $A, B, C, D$  are incidence matrices for the Morse functions in the four regions in the parameter space separated by the parameter values of cubic singularities as indicated in Figure 4.6.

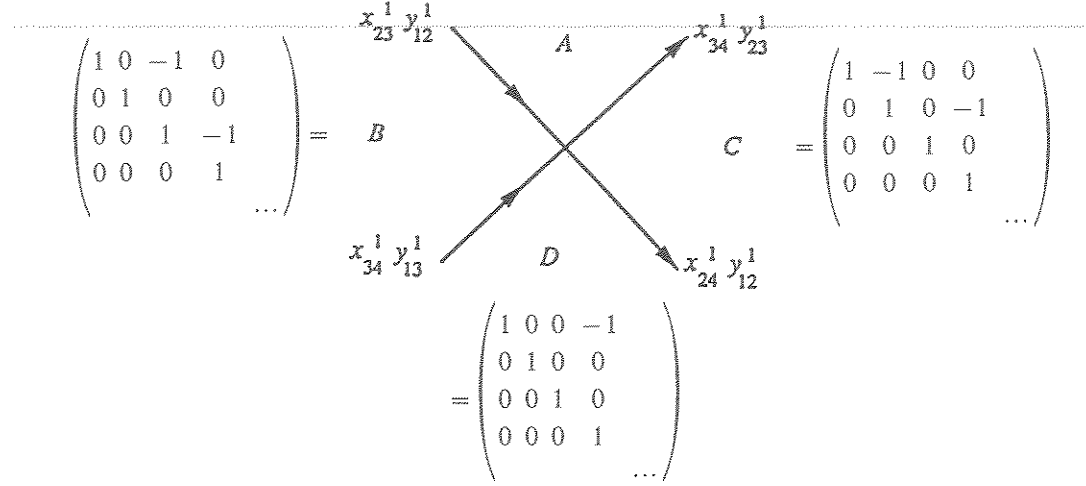


Fig. 4.6.

All four matrices have the property that their  $(3, 2)$ -entries are 0. The exchange relation  $Z_{23}^1(X)$  gives (14) with  $r = 1$  for  $X = A$  and (17), (18), (19) below for  $X = B, C, D$ .

$$BE_{23}(1)E_{24}(-1) = E_{23}(1)B, \quad (17)$$

$$CE_{23}(1) = E_{13}(-1)E_{23}(1)C, \quad (18)$$

$$DE_{23}(1) = E_{23}(1)D. \quad (19)$$

This gives four different ways to get from (15) to (16) as indicated below

- (a)  $y_{12}^{-1}x_{23}^{-1}x_{34}^1y_{23}^1 \rightarrow_{(14)} y_{12}^{-1}x_{23}^{-1}(x_{23}^1x_{24}^{-1}y_{13}^1y_{23}^{-1})x_{34}^1y_{23}^1$   
 $= y_{12}^{-1}x_{24}^{-1}y_{13}^1y_{23}^{-1}x_{34}^1y_{23}^1 \sim x_{34}^1y_{12}^{-1}y_{13}^1x_{24}^{-1} \sim x_{34}^1y_{13}^1y_{12}^{-1}x_{24}^{-1}$
- (b)  $y_{12}^{-1}x_{23}^{-1}x_{34}^1y_{23}^1 \rightarrow_{(17)} (x_{23}^1x_{24}^{-1}y_{23}^{-1})y_{12}^{-1}x_{23}^{-1}x_{34}^1y_{23}^1$   
 $\sim x_{34}^1y_{23}^{-1}y_{12}^{-1}y_{23}^1x_{24}^{-1} \sim x_{34}^1y_{13}^1y_{12}^{-1}x_{24}^{-1}$
- (c)  $y_{12}^{-1}x_{23}^{-1}x_{34}^1y_{23}^1 \rightarrow_{(18)} (y_{12}^{-1}x_{23}^{-1}x_{34}^1y_{23}^1)(x_{23}^1y_{23}^{-1}y_{13}^1)$   
 $\sim x_{34}^1y_{12}^{-1}y_{13}^1x_{24}^{-1} \sim x_{34}^1y_{13}^1y_{12}^{-1}x_{24}^{-1}$
- (d)  $y_{12}^{-1}x_{23}^{-1}x_{34}^1y_{23}^1 \sim x_{34}^1y_{12}^{-1}x_{23}^{-1}y_{23}^1x_{24}^{-1} \sim x_{34}^1y_{13}^1(x_{23}^{-1}y_{23}^1)y_{12}^{-1}x_{24}^{-1}$   
 $\rightarrow_{(19)} x_{34}^1y_{13}^1y_{12}^{-1}x_{24}^{-1}.$

In each case, we used Steinberg relations first among the  $x_{ij}$ 's and then among the  $y_{ij}$ 's.

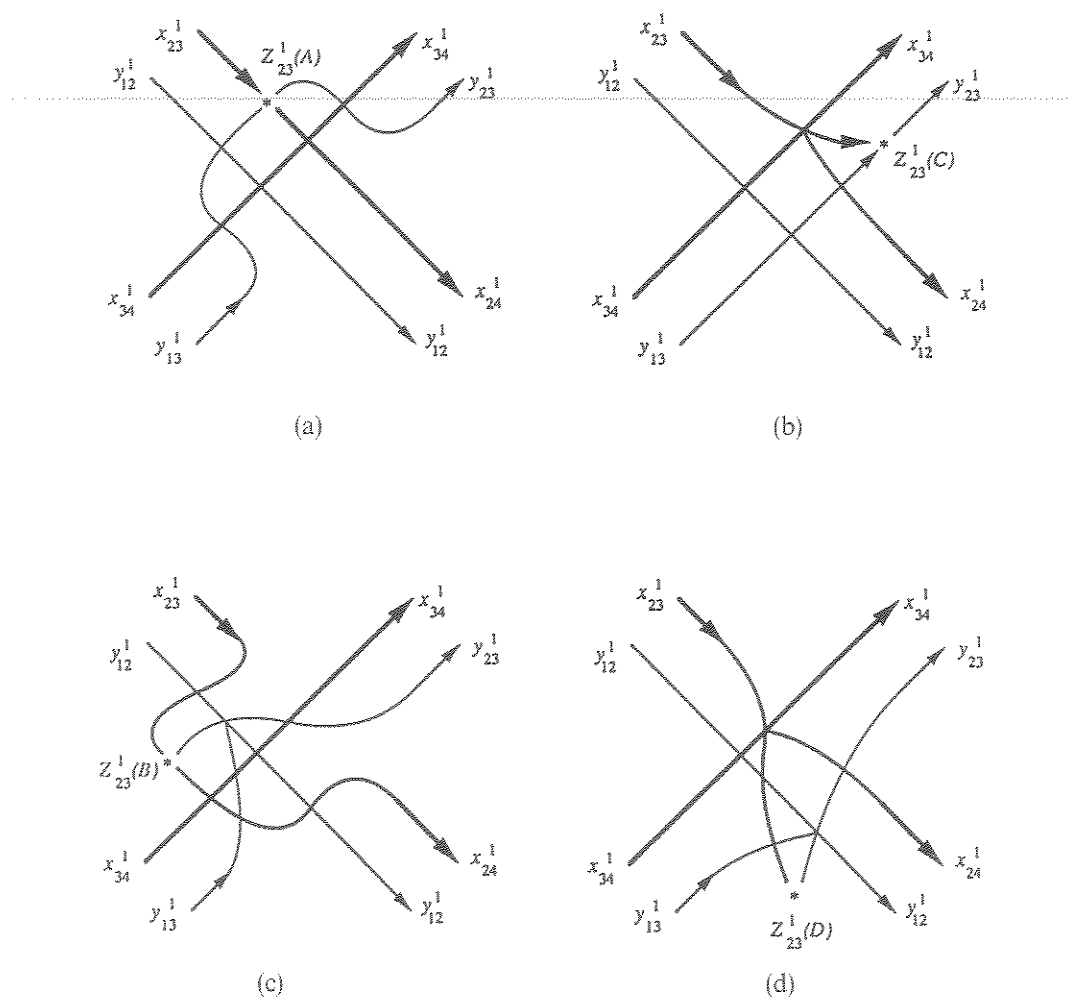


Fig. 4.7.

The algebraic deformations given above can be represented by the 'partial generalized pictures' given in Figure 4.7. Fortunately all four diagrams are equivalent. (They can be deformed into each other.) This is because they involve only those elementary operations and exchange relations which are 'compatible' with the ordering given in (13) above. The definition of compatibility is given as follows.

**DEFINITION 4.8.** Let  $<$  be a partial ordering of the set  $\{x_1, \dots, x_m, y_1, \dots, y_n\}$ . Then the  $n \times m$  matrix  $A$ , the column operation  $x_{ab}^c$ , row operation  $y_{cd}^s$  and exchange

relation  $Z_{pq}^i$  are said to be *compatible* with the ordering  $<$  if, respectively,

- (1)  $a_{ij} = 0$  whenever  $x_j < y_i$ ,
- (2)  $x_a < x_b$ ,
- (3)  $y_c < y_d$ ,
- (4)  $x_p < y_q$ .

For the partial ordering (13) the compatible operations are  $x_{ab}^i$  where  $2 \leq a < b \leq 4$ ,  $y_{cd}^s$  where  $1 \leq c < d \leq 3$  and  $Z_{23}^i$ . A matrix  $A$  is compatible with (13) if and only if  $a_{32} = 0$ .

We note that any compatible operation on a compatible matrix results in a compatible matrix and all elementary operations involved in a compatible exchange relation are compatible assuming we have a fixed partial ordering.

### 5. The Hopf Bundle $S^3 \rightarrow S^2$

We will now construct a fiberwise PGMF on the Hopf bundle  $p: S^3 \rightarrow S^2$ . As before the first step is to construct a system of embedded disks. This is illustrated in Figure 5.1.

The first disk  $D_1$  appears as a spiral since it covers the point at infinity in  $S^2 = \mathbb{R}^2 \cup \{\infty\}$ . The image of the three disks in  $S^2$  is given in Figure 5.2 where  $pD_1$

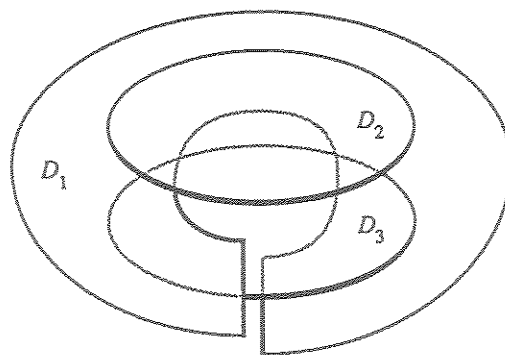


Fig. 5.1.

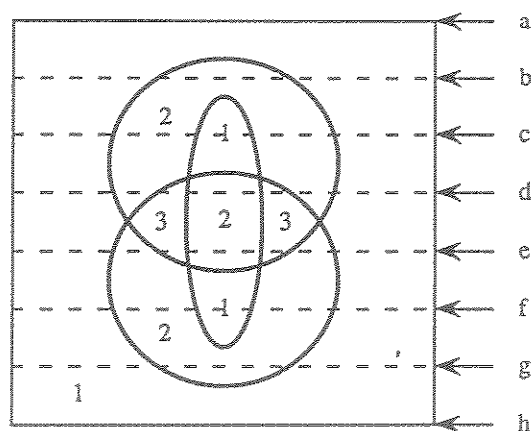


Fig. 5.2.

is the complement of the innermost oval. The numbers 1, 2, 3 in Figure 5.2 indicate the number of times each region in  $S^2$  is covered by a disk.

The cross-sections of Figure 5.1 at the levels (a)–(h) indicated in Figure 5.2 are illustrated in Figure 5.3. The corresponding configurations of critical points are indicated in Figure 5.4.

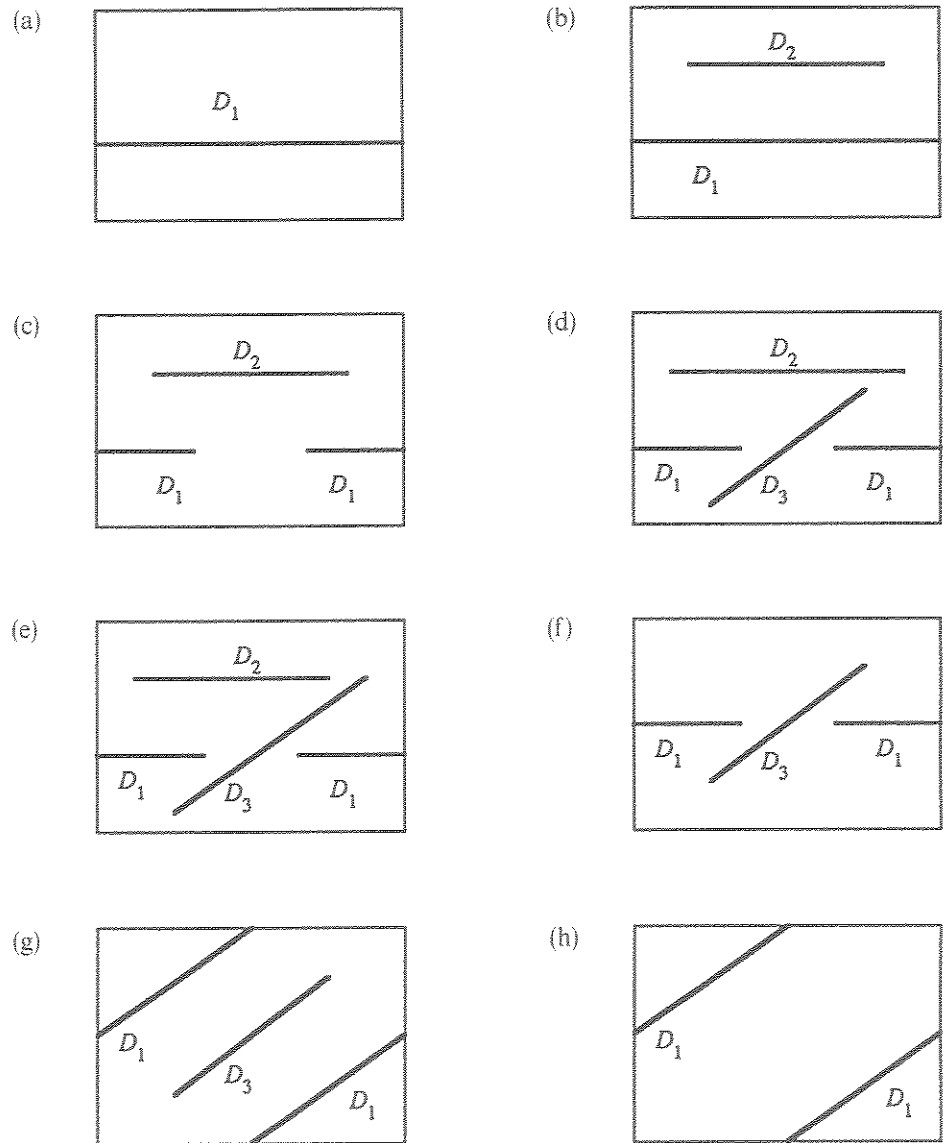


Fig. 5.3.

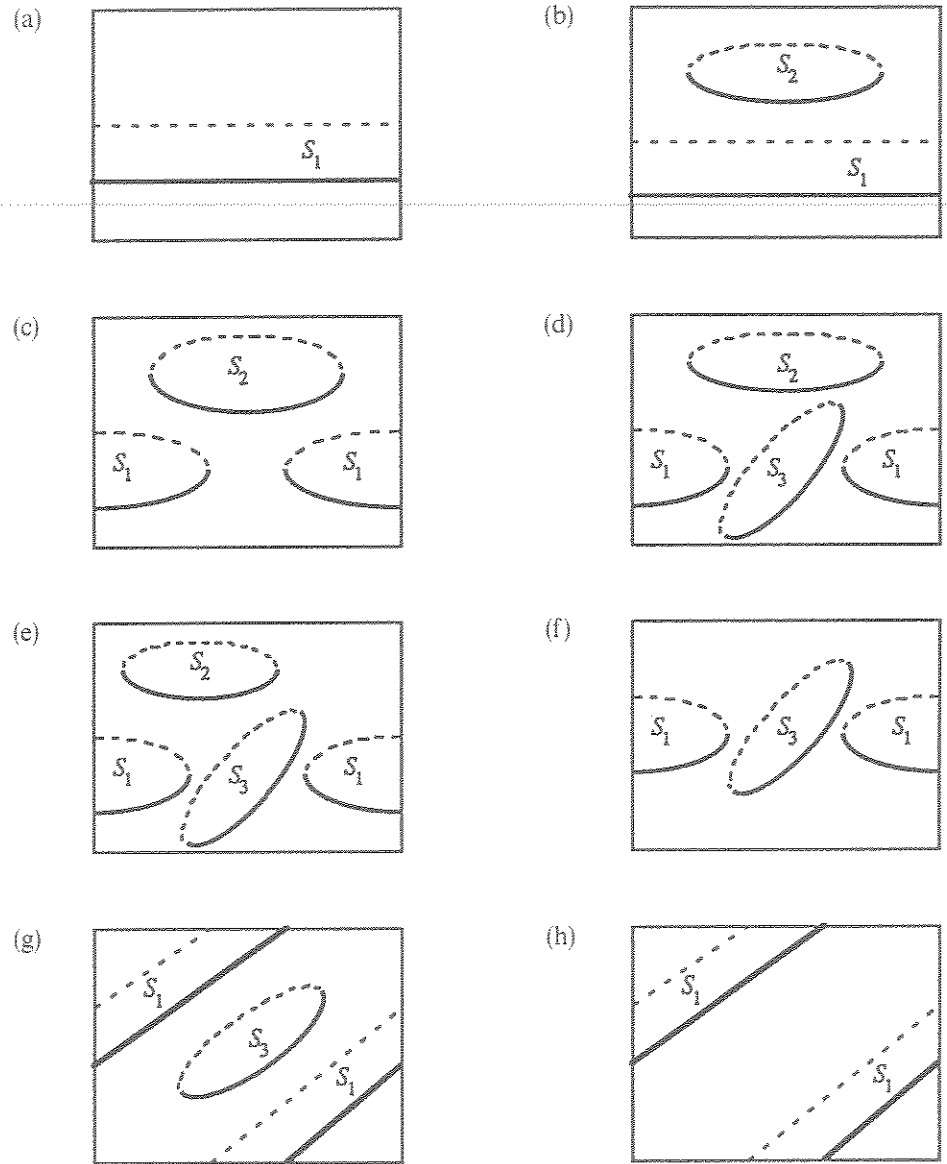


Fig. 5.4.

As in Section 2, each cubic point on the  $i$ th sphere leads to one column operation  $x_{ij}$  and one row operation  $y_{ki}$ , where  $j, k$  are the numbers of the spheres directly counterclockwise and clockwise from  $S_i$  at the cubic point. Thus, each circle in Figure 5.2 leads to two circles of elementary operations as illustrated in Figure 5.5. At each of the six crossings of cubic points we insert one copy of Figure 4.7(c), the simplest of the four equivalent choices for filling in the diagram at these points.

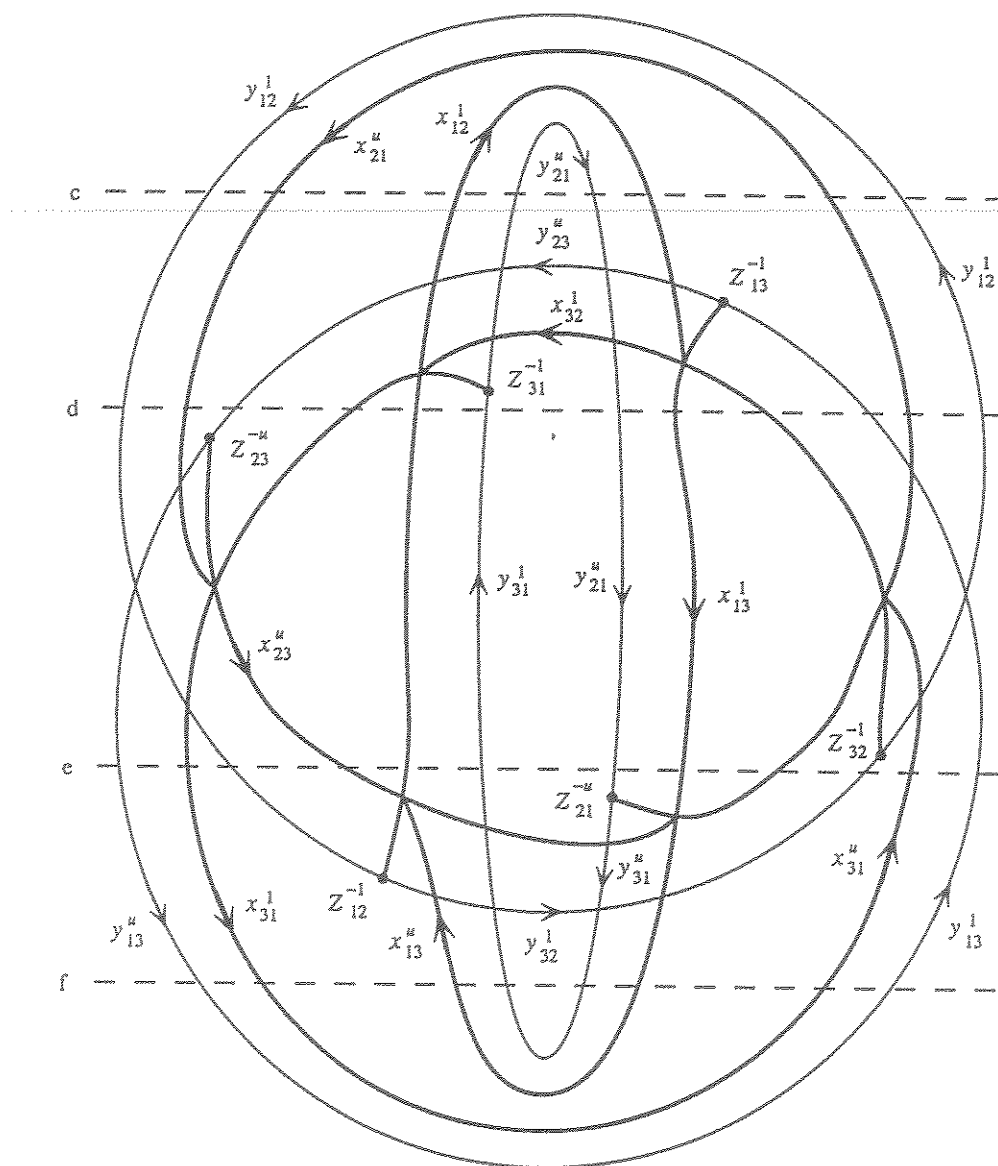


Fig. 5.5.

According to the procedure explained in Section 2, the diagrams (c), (d), (e), (f) in Figures 5.3 and 5.4 lead to the following sequences of elementary operations which form the corresponding cross-sections of Figure 5.5.

$$(c) \quad y_{12}^{-1} x_{21}^{-u} x_{12}^1 y_{21}^u y_{21}^{-u} x_{12}^{-1} x_{21}^u y_{12}^1,$$

$$(d) \quad y_{12}^{-1} x_{21}^{-1} y_{23}^{-1} x_{31}^{-1} x_{12}^1 y_{31}^1 y_{21}^{-u} x_{13}^{-1} x_{32}^1 y_{13}^1 x_{21}^u y_{12}^1,$$

$$(e) \ y_{13}^{-u} x_{31}^{-1} y_{12}^{-1} x_{23}^{-u} x_{12}^1 y_{31}^1 y_{21}^{-u} x_{13}^{-1} x_{21}^u y_{32}^1 x_{31}^u y_{13}^1,$$

$$(f) \ y_{13}^{-u} x_{31}^{-1} x_{13}^u y_{31}^1 y_{31}^{-u} x_{13}^{-1} x_{31}^u y_{13}^1.$$

Except in the case  $u = 1$ , the cross-section (g) does not have a well-defined sequence of elementary operations associated to it since the critical points on  $S_1$  pass through the base point (the top and bottom horizontal lines in the rectangles in Figures 5.3, 5.4). As a consequence the elementary operations labeling the solid lines do not match below the cross section (f) in Figure 5.5 (unless  $u = 1$ ). Aside from this problem we are, as usual, using our 'smooth edge' convention which says that all portions of any smoothly embedded curve have the same label except at exchange points.

The problem with the labels in 5.5 can be attributed to the fact that the local coefficient system on the circles does not extend to one on  $E = S^3$  unless  $u = 1$ .

If we want a nontrivial local coefficient system on each circle which extends to  $E$  we must take the lens space  $E = S^3/(\mathbb{Z}/n) = L(n; 1, 1)$ . Then we can take  $u$  to be any  $n$ th root of 1 in any commutative ring  $R$ . (Noncommutative rings work if we take right  $R$ -modules.) In this case we can again find a system of three disjoint 2-disks as indicated in Figures 5.6 and 5.7 for the case  $n = 3$ . These diagrams are analogous to Figures 5.2 and 5.3.

In Figure 5.7(c) and (d) the three pieces of the disk  $D_3$  are labelled  $D_3, uD_3, u^2D_3$  since, e.g., the second piece actually belongs to the next lower fundamental region. This allows us to connect the three pieces as shown in 5.7(e). When the basis elements  $x_3, y_3$  are replaced by  $ux_3, uy_3$  then the incidence matrix  $A$  with respect to the new basis is the same as  $DAD^{-1}$  with respect to the original basis where  $D = \text{diag}(1, 1, u)$ . Thus, e.g., the sequence of elementary operations for 5.7(d) is  $E(DED^{-1})(D^2ED^{-2})$  where  $E$  is given by 5.4(f) above. If we expand this, we get

$$\begin{aligned} & (y_{13}^{-u} x_{31}^{-1} x_{13}^u y_{31}^1 y_{31}^{-u} x_{13}^{-1} x_{31}^u y_{13}^1) (y_{13}^{-1} x_{31}^{-u} x_{13}^1 y_{31}^u y_{31}^{-u^2} x_{13}^{-u^{-1}} x_{31}^{u^2} y_{13}^{u^{-1}}), \\ & (y_{13}^{-u^{-1}} x_{31}^{-u^2} x_{13}^{u^{-1}} y_{31}^{u^2} y_{31}^{-u^3} x_{13}^{-u^{-2}} x_{31}^{u^3} y_{13}^{u^{-2}}). \end{aligned} \quad (20)$$

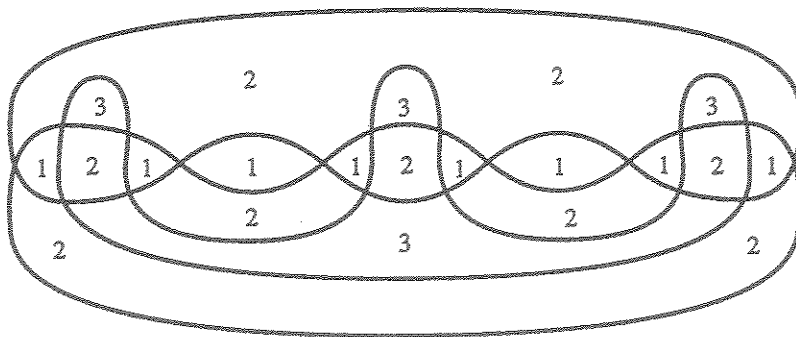


Fig. 5.6.

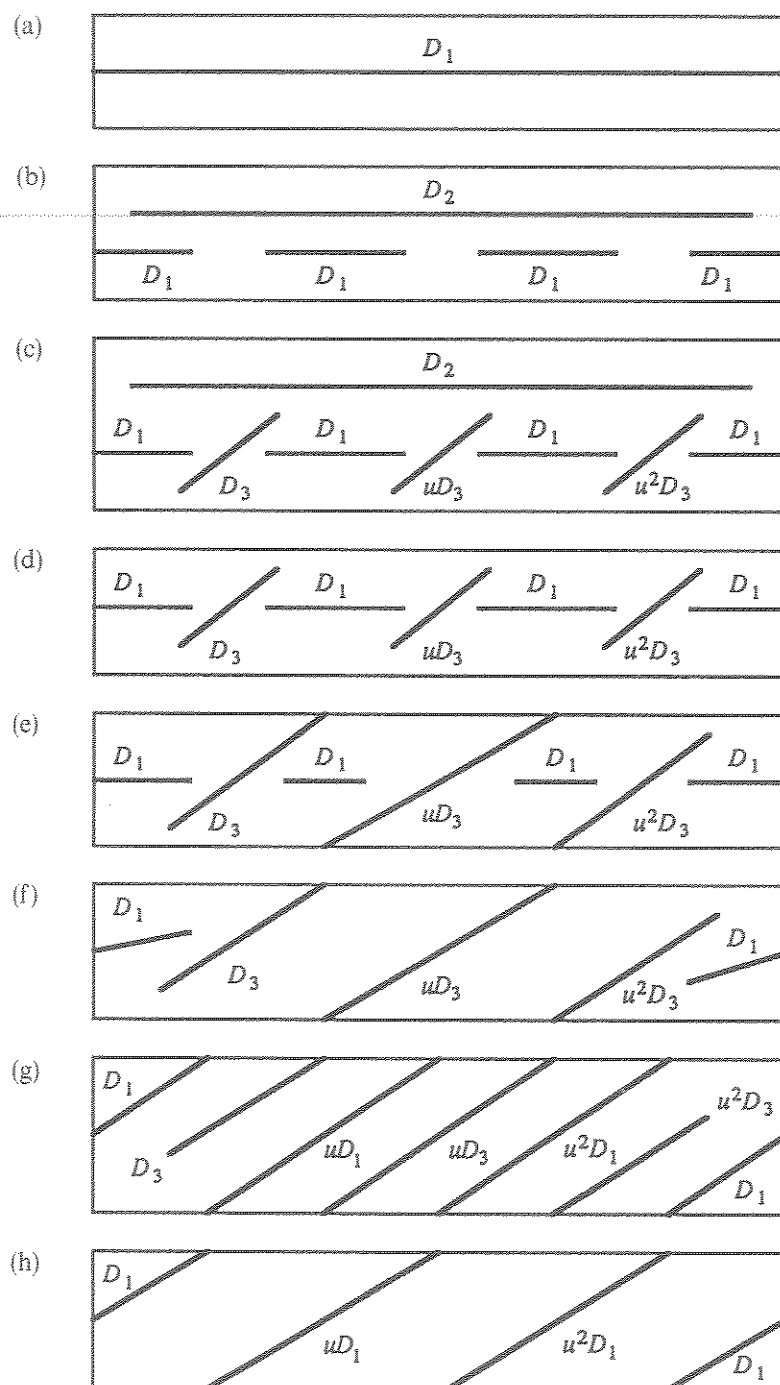


Fig. 5.7.

Most of these terms cancel to give

$$y_{13}^{-u} x_{31}^{-1} x_{13}^u y_{31}^1 y_{31}^{-u^3} x_{13}^{-u^{-2}} x_{31}^{u^3} y_{13}^{u^{-2}}, \quad (21)$$

which is trivial since  $u^3 = 1$ .

We note that (21) is the sequence of elementary operations for 5.7(f). Geometrically, the deformation 5.7(d)  $\rightarrow$  (e)  $\rightarrow$  (f)  $\rightarrow$  (g)  $\rightarrow$  (h) has no crossings of cubic points. This is why algebraically the terms in (20) all cancel without using any Steinberg or exchange relations.

Since algebraically diagram 5.7 is  $n$  copies of 5.3, the resulting picture should be  $n$  copies of the picture 5.5 conjugated by  $D^i$  and connected together as shown in Figure 5.8 where  $P$  is the portion of Figure 5.5 which lies between the cross-sections (c) and (f). Note that Figure 5.8 can be deformed to Figure 5.9 since the lines at the top do not involve the index 3 so they are unchanged by conjugation by  $D$ . To get a true picture of an element of  $K_3R$  we need to eliminate all row operations in Figure 5.9. By the  $n$ -fold symmetry of Figure 5.9 this can be done by working with Figure 5.5 if we are careful.

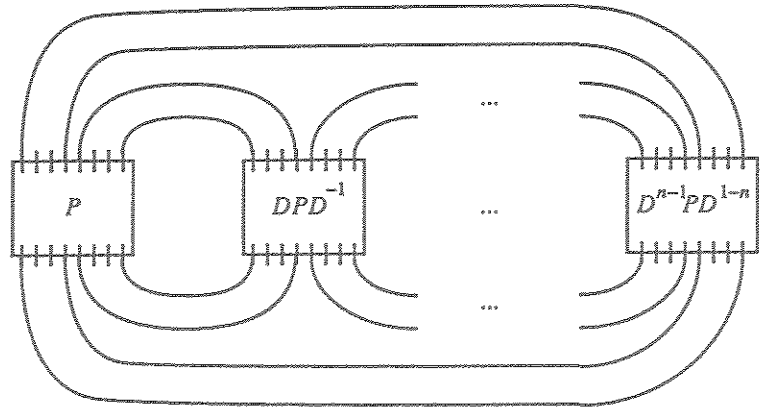


Fig. 5.8.

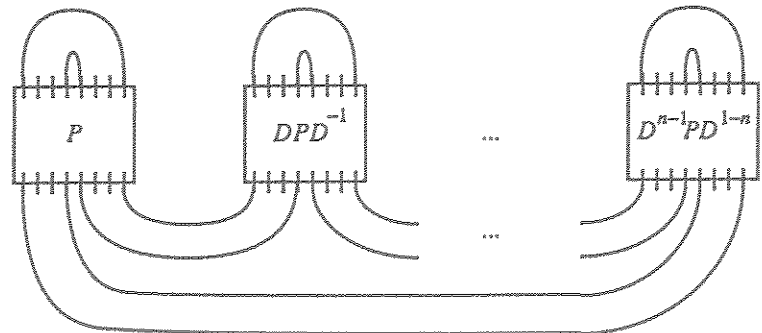


Fig. 5.9.

## 6. Elimination of Row Operations

In this section, we will show how Figure 5.9 can be deformed to give the picture  $L_n$  of Part A. We begin by summarizing the results in [7] related to the elimination of row operations in a 'generalized picture' involving both row and column operations.

A *generalized picture* for  $K_3$  is a one-dimensional planar diagram in which the regions are labeled with elements of  $GL(R)$ , the edges are oriented and labelled with row and column operations so that the matrix labels on the two regions separated by an edge differ by the elementary operation labeling the edge as indicated in (22).

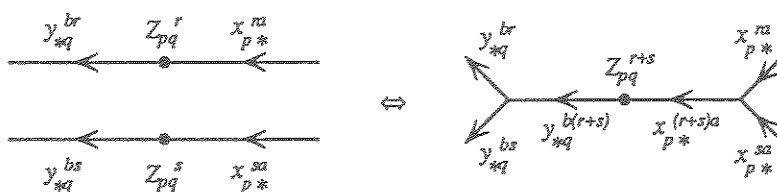
$$\begin{array}{ccc} E_{pq}(s)A & \downarrow & A \uparrow AE_{ij}(r) \\ y_{pq}^s & & x_{ij}^r \end{array} \quad (22)$$

At each vertex the labels on the edges converging to the vertex, when read counter-clockwise, should give either a Steinberg relation among  $x_{ij}$ 's or  $y_{ij}$ 's (or an inverse of a Steinberg relation) or a commutator  $[x_{ij}^r, y_{qp}^s]$  or an exchange relation. All three occur in Figure 5.5. (Noncommuting Steinberg relations among the  $y_{ij}$ 's occur in Figure 4.7.)

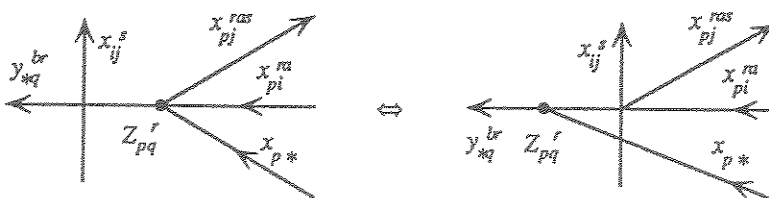
A *local deformation* of a generalized picture is given as follows. First we choose an open subset of the plane in which all the labels are compatible with a fixed partial ordering of the set  $\{x_1, y_1, x_2, y_2, \dots\}$  as defined in 4.8. Then we change the generalized picture inside  $U$  so that it is still compatible with the chosen partial ordering. (We must of course keep it the same near the boundary of  $U$  so that it matches the rest of the picture.) A *deformation* of a generalized picture is a sequence of local deformations.

There are basically three kinds of local deformations involving exchange points. They are:

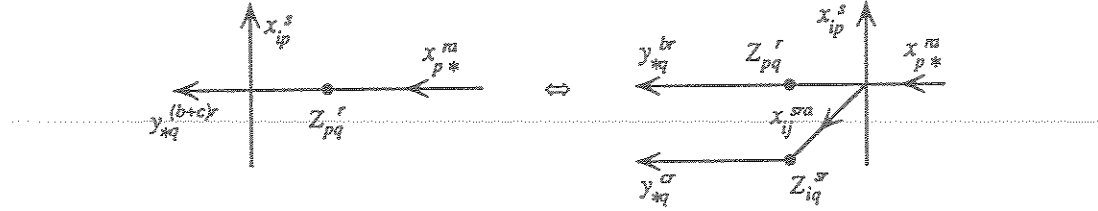
Type I  $Z_{qp}^r(A) + Z_{qp}^s(A) \Leftrightarrow Z_{qp}^r + s(A):$



Type IIa  $Z_{qp}^r(A) \Leftrightarrow Z_{qp}^r(Ax_{ij}^s)$  if  $j \neq p$ :



Type IIIa  $Z_{qp}^r(Ax_{ip}^s) \Leftrightarrow Z_{qp}^r(A) + Z_{iq}^s(A)$ :



There are also dual versions IIb, IIIb of IIa, IIIa with row operations given by

$$(IIb) \quad Z_{qp}^r(A) \Leftrightarrow Z_{qp}^r(y_{ij}^s A) \quad \text{if } i \neq q,$$

$$(IIIb) \quad Z_{qp}^r(y_{qj}^{-s} A) \Leftrightarrow Z_{qp}^r(A) + Z_{pj}^{rs}(A).$$

The main result about generalized pictures is the following theorem which was proved in [7] in the special case when  $R$  is an integer group ring.

**THEOREM 6.1.** *Any generalized picture can be deformed into a picture without row operations. Furthermore the element of  $K_3 R$  represented by the resulting (true) picture is well defined.*

*Remark.* This theorem does not say that the group of deformation classes of generalized pictures is isomorphic to  $K_3 R$ . It is instead isomorphic to  $K_1 R \times K_3 R$ . The  $K_1 R$ -invariant is given by the matrix label on any region. The group operation for deformation classes of generalized pictures is given by disjoint union of diagrams and direct sum of matrix labels.

*Proof.* We give only the conceptual outline of the proof. For details of the deformation removing the row operations see [7], Theorem 9.3. This step works just as well for any ring  $R$ . For details of the uniqueness of the resulting element of  $K_3 R$ , see [10].

First we note that any permutation matrix  $P$  gives an automorphism of the set of deformation classes of generalized pictures by changing all matrix labels  $A$  to  $PA$  and by conjugating all row operations by  $P$ . Therefore we may assume that  $p \neq q$  for each exchange relation  $Z_{qp}^r$  which occurs in our generalized picture  $L$ .

We also observe that there is an action of  $K_1 R$  on the group of all deformation classes of generalized pictures given by direct sum with the matrix labels. Therefore we may assume that the  $K_1 R$ -invariant of  $L$  is trivial. In fact by local deformations at  $\infty$  we may assume that the unique unbounded region of  $L$  is labelled with the identity matrix.

Next we claim that we can deform all the exchange relations in  $L$  so that they occur at the identity matrix. (This is Lemma 9.1 in [7].) To see this let  $Z_{qp}^r(A)$  be an exchange relation in  $L$ . Then, since  $p \neq q$  and  $A$  is trivial in  $K_1 R$ , there is a sequence of row and column operations which commute with  $Z_{qp}^r$  as in IIa, b above and which transform  $A$  into  $I$ . One can then perform these operations one at a time by creating a circle of elementary operations next to the exchange point and then pass the exchange point through the circle to its interior by a Type II deformation. (See Figure 6.2.)

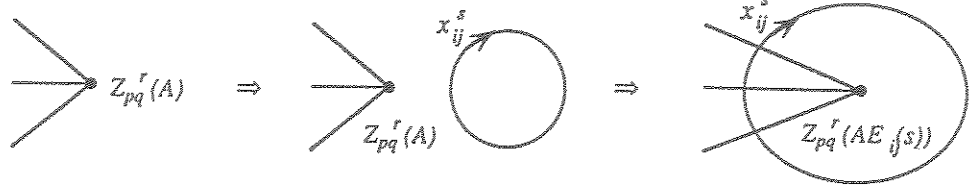


Fig. 6.2.

Finally, when all the exchange points are exterior we can exchange the remaining row operations by 'sliding them out' to the unbounded region and exchanging them up when they get there. This is merely the two-dimensional version of the deformation

$$E_n \dots E_1 I F_1 \dots F_m \Rightarrow E_n \dots E_2 I E_1 F_1 \dots F_m \Rightarrow I E_n \dots E_1 F_1 \dots F_m$$

which slides any sequence of row operations into column operations one at a time by exterior exchanges.

To prove that the resulting picture gives a well defined element of  $K_3 R$  we use the filtered complex model for  $\Omega K(R)$  given in [10]. There is a Waldhausen category  $\mathcal{K}(R)$  whose objects are filtered  $R$ -complexes with certain additional structure. A partial ordering of the set  $\{x_1, \dots, x_n, y_1, \dots, y_m\}$  and a compatible  $m \times n$  matrix  $A$  gives a filtration for the chain complex  $\dots \rightarrow 0 \rightarrow R^n \rightarrow R^m$  with boundary map given by  $A$ . This means that every generalized picture gives a map  $S^2 \rightarrow |\mathcal{K}^h(R)|$  where  $\mathcal{K}^h(R)$  is the category of weak equivalences among acyclic filtered chain complexes. (Actually the natural map sends  $S^2$  to something which continues  $|\mathcal{K}^h(R)|$  as a deformation retract.) By 'rigidity' of the basis set (i.e. we are not allowed to permute the basis), we are actually in the fiber of the map  $|\mathcal{K}^h(R)| \rightarrow |\mathcal{K}(R)|$ . This maps to the homotopy fiber of the map

$$\Omega |\mathcal{K}^h(R)| \rightarrow \Omega |\mathcal{K}(R)|.$$

This homotopy fiber, say  $F$ , is homotopy equivalent to

$$\Omega^2 |\mathcal{K}(R)| \simeq \Omega K(R),$$

where  $K(R)$  denotes  $BGL(R)^+ \times K_0 R$ .

It now remains to show that the map from  $K_3 R = \pi_2 \Omega K(R)$  to  $\pi_2 F$  given by going from pictures to generalized pictures to  $\pi_2 F$  by the construction above is an isomorphism. This follows from the fact that picture are elements of  $\pi_2$  of the Volodin model for  $\Omega K(R)$  and the map in question is induced by a map  $\Omega K(R) \rightarrow F \simeq \Omega K(R)$  which is equivariant with respect to an appropriate free action of  $GL(R)$ . Then we invoke the obvious fact that any  $GL(R)$  equivariant map between two models for  $\Omega K(R)$  must be a weak homotopy equivalence. (This follows by induction on the Postnikov tower of  $ZK(R)/GL(R)$  and the universality of each of its Postnikov invariants.)  $\square$

We will now perform a deformation to simplify Figure 5.5. Since the labels below the cross section (f) do not match we will only consider the portion of Figure 5.5 above the cross section (f).

The first step is to move the  $y_{21}^u$  edge down until it is a straight line connecting the exchange points  $Z_{31}^{-1}$  and  $Z_{21}^u$ . This is allowed since  $y_{21}^u$  commutes with  $y_{23}^u$  and any  $x_{ij}$ . Next we move the two exchange points  $Z_{31}^{-1}$  and  $Z_{21}^u$  down through the  $x_{23}^u$  edge by a type IIa deformation. This produces a single  $Z_{31}^{-1}$  exchange below the  $x_{23}^u$  line as indicated in the lower portion of Figure 6.3.

The third step is to move the  $y_{23}^u$  edge up above the  $x_{12}^1$  edge. Then the two exchange points  $Z_{23}^u$  and  $Z_{13}^{-1}$  can be pushed up past the  $x_{21}^u$  edge by another type IIa deformation. Figure 6.3 shows the result of these four local deformations.

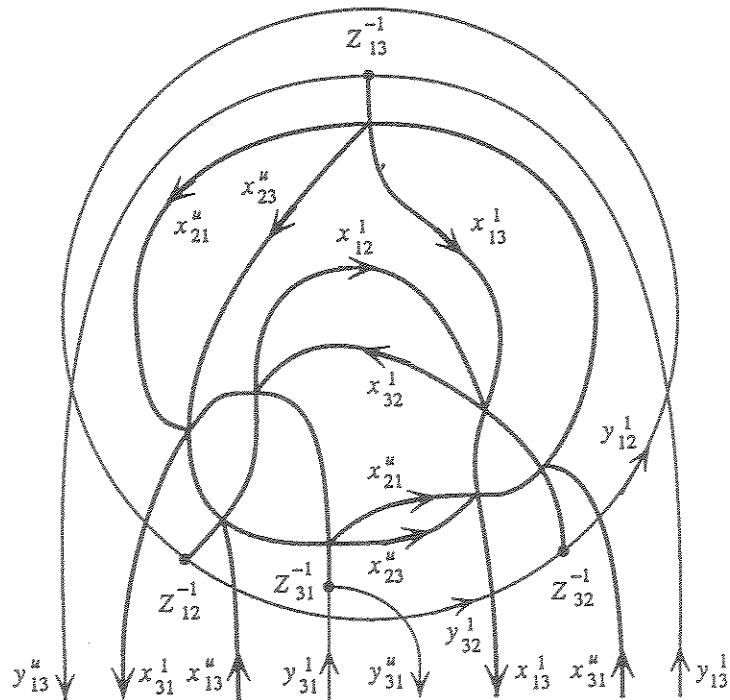


Fig. 6.3.

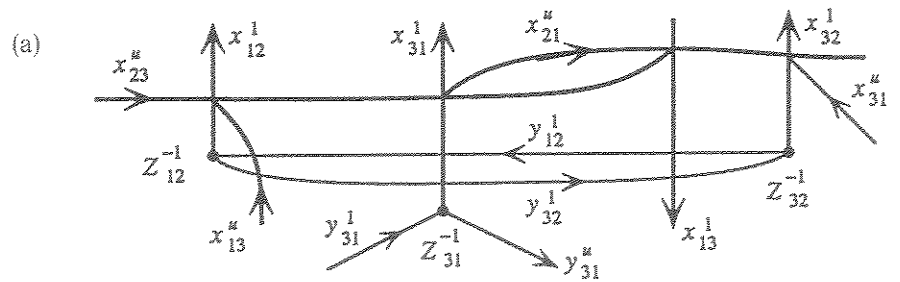


Fig. 6.4.

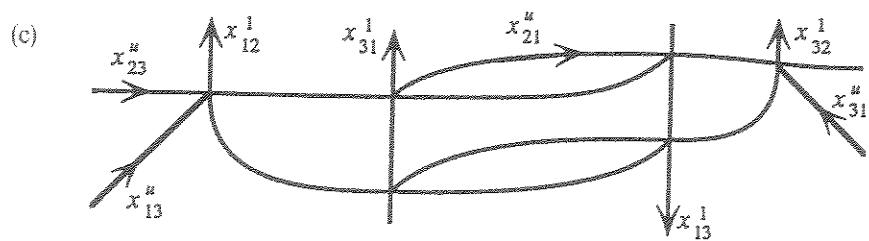
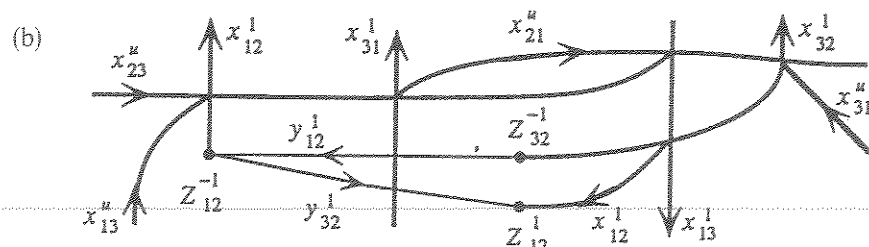


Fig. 6.4. Cont.

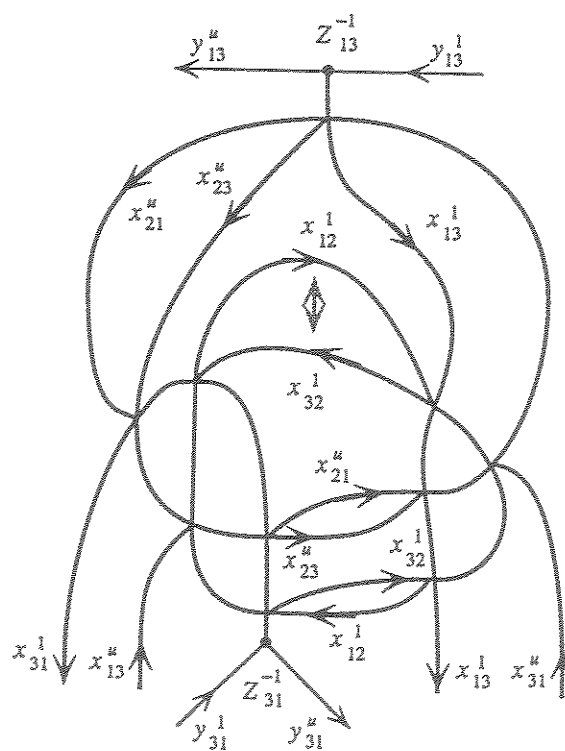


Fig. 6.5.

Now we want to cancel the two exchange points  $Z_{12}^{-1}$  and  $Z_{32}^{-1}$ . To do this we first push the  $y_{12}^1$  edge down so that it forms a straight line from  $Z_{12}^{-1}$  to  $Z_{32}^{-1}$ . This is a combination of deformation IIb and commutation of  $y_{12}^1$  with various  $x_{ij}$ 's. Next we push the  $Z_{31}^{-1}$  exchange down below the  $y_{32}^1$  edge by a type IIb deformation. This gives Figure 6.4(a).

To get from 6.4(a) to 6.4(b) we do a type IIa deformation on  $Z_{12}^{-1}$  and a type IIa deformation on  $Z_{32}^{-1}$ . We also redraw the  $[x_{23}^u, x_{12}^1]$  Steinberg relation for aesthetic reasons. To get from 6.4(b) to 6.4(c) we do a type IIa deformation. If we now insert 6.4(c) back into 6.3 we get Figure 6.5.

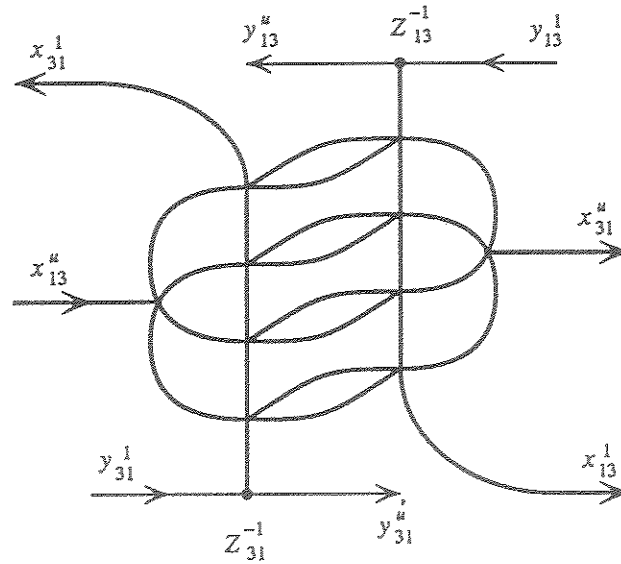


Fig. 6.6.

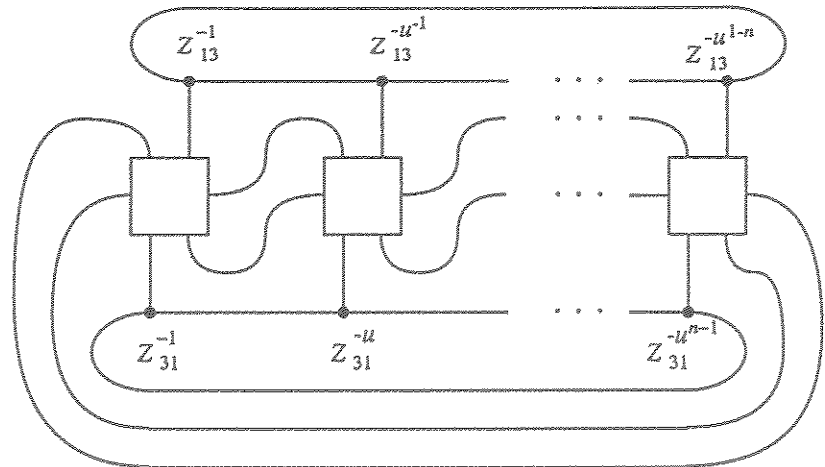


Fig. 6.7.

If we deform Figure 6.5 by an isotopy of the plane and interchange the positions of  $x_{12}^1$  and  $x_{32}^1$  as indicated by the double arrows we will get Figure 6.6 which is almost the same as Figure 2.1 in Part A.

When Figure 5.5 (the portion above (f)) is deformed to Figure 6.6 the entire picture (Figure 5.9) is deformed to Figure 6.7. We can now see that there are two strings of exchange points which cancel by deformations of type I since  $1 + u + \dots + u^{n-1} = 0$ . This deforms Figure 6.7 into the picture  $L_n$  (Figure 2.2 in Part A). To make a perfect match we should rotate each square in 6.7 counterclockwise by  $\pi/2$ .

## 7. Higher Reidemeister Torsion

The association of  $D_2(\xi)$  to the circle bundle  $L(n; 1, 1) \rightarrow S^2$  is a special case of a more general construction called 'higher Reidemeister torsion'. Instead of  $S^1$  let  $M$  be any smooth closed manifold. Let  $\rho$  be a unitary representation of  $\pi_1 M$  whose image is a finite subgroup of  $U(n)$  and suppose that  $H_*^{\rho}(M, \mathbb{C}^n) = 0$ , i.e. the homology of  $M$  with coefficients in the flat  $\mathbb{C}^n$ -bundle corresponding to  $\rho$  is trivial. Suppose that  $M \rightarrow E \rightarrow S^{2k}$  is a smooth bundle so that the unitary representation  $\rho$  of  $\pi_1 M$  factors through  $\pi_1 E$ . (This is the same as taking an element of  $\pi_{2k-1} \text{Diff}(M)$  when  $k \geq 2$  or of a certain subgroup of  $\pi_1 \text{Diff}(M)$  when  $k = 1$ .)

Then there is an  $\mathbb{R}$ -valued invariant  $\tau(E)$  which is additive (i.e.  $\tau: \pi_{2k-1} \text{Diff}(M) \rightarrow \mathbb{R}$  is a homomorphism on its domain). In the relative case (when  $M$  is a manifold with boundary) the known results from pseudoisotopy theory tell us that  $\tau$  detects fiber homotopically trivial but smoothly nontrivial bundles over every even dimensional sphere. In the case of bundles over  $S^2$  the argument goes as follows.

We take a smooth manifold  $M$  of sufficiently large dimension ( $\geq 6$ ) with  $\pi_1 M = \mathbb{Z}/p$  and  $\pi_2 M = 0$ , e.g.  $M = L \times I$  where  $L$  is the lens space  $L = L(p, 1, 1, 1) = S^5/(\mathbb{Z}/p)$  where  $p$  is an odd prime. Then by the surjective stability theorem ([7], [9])  $\pi_1 \mathcal{C}(M)$  maps onto  $\text{Wh}_3(\mathbb{Z}/p)/\text{torsion} \approx K_3 \mathbb{Z}[\mathbb{Z}/p]/\text{torsion} \approx K_3 \mathbb{Q}(\xi)/\text{torsion}$  where  $\mathcal{C}(M)$  is the concordance space

$$\mathcal{C}(M) = \text{Diff}(M \times I \text{ rel } M \times 0 \cup \partial M \times I).$$

Consequently there is an element of  $\pi_1 \mathcal{C}(M)$  which is detected by  $\tau$  which is the composition of the Borel regulator map  $K_3 \mathbb{Q}(\xi) \rightarrow \mathbb{R}$  with the map described above. (In fact, we know from the results of this paper that we can get  $\tau = pD_2(\xi)$ .)

Since  $M$  is an even dimensional manifold which is sufficiently tangentially trivial (in this case orientable) the involution on  $\pi_1 \mathcal{C}(M)$  given by 'turning Morse functions upside down' acts as the negative of the inverse conjugate transpose on  $K_3 \mathbb{Q}(\xi)$  and thus preserves the invariant  $\tau$  by Corollary 7.3 below. Consequently we can construct an element of  $\pi_1 \text{Diff}(M \times I \text{ rel } \partial(M \times I))$  which is detected by  $\tau$  (in fact with  $\tau = 2pD_2(\xi)$ ). By pasting this into the closed manifold  $L \times S^2$  we get a smooth bundle over  $S^2$  with fiber  $L \times S^2$  detected by  $\tau$ . This proves the following.

**THEOREM 7.1.** *Let  $L = L(p, 1, 1, 1) = S^5/(\mathbb{Z}/p)$  where  $p$  is an odd prime. Let  $\rho: \pi_1(L \times S^2) = \mathbb{Z}/p \rightarrow U(1)$  be any nontrivial map. Then there is a smooth bundle  $E \rightarrow S^2$  with fiber  $L \times S^2$  and  $\pi_1 E = \mathbb{Z}/p$  so that its higher Reidemeister torsion invariant  $\tau(E)$  is nontrivial. Furthermore  $E$  is fiber concordant to (and a fortiori fiber homotopy equivalent to) the trivial bundle  $L \times S^2 \times S^2 \rightarrow S^2$ , i.e. there is a smooth bundle  $W \rightarrow S^2$  with fiber  $L \times S^2 \times I$  so that  $\partial W$  is fiber diffeomorphic to  $E \amalg L \times S^2 \times S^2$ .  $\square$*

The calculation in this paper shows that this invariant also detects circle bundles over  $S^2$  which, of course, are classified by fiber homotopy type.

**THEOREM 7.2.** *The higher Reidemeister torsion of the  $S^1$ -bundle  $L(n, 1, 1) \rightarrow S^2$  is  $nD_2(\xi)$ , where  $\xi$  is the inverse of the holonomy of the coefficient sheaf over each fiber.*

*Remark.* In order to show that the invariant in this paper is a special case of the more general higher Reidemeister torsion of [10–12] we need an equivalence between two different models for  $\Omega K(R)$  as outlined in the proof of Theorem 6.1.  $\square$

Since  $S^1$  is an oriented closed odd dimensional manifold this theorem has the following  $K$ -theoretic corollary (although the corollary could also be obtained by direct computation).

**COROLLARY 7.3.** *Let  $t$  be the involution on  $K_3\mathbb{Z}[\xi]$  given by inverse conjugate transpose on matrices. Then  $t = -1$  on  $K_3\mathbb{Z}[\xi]/\text{torsion}$ .*

*Proof.* Let  $E \rightarrow S^2$  be a circle bundle and let  $\rho: \pi_1 E \rightarrow U(1)$  be a unitary representation so that  $(E, \rho)$  represents a nontrivial element of  $K_3\mathbb{Z}[\xi]/\text{torsion}$ . Let  $f: E \rightarrow \mathbb{R}$  be a PGMF on  $E$ . Then  $-f$  is also a PGMF on  $E$  if we reverse the orientations of all the fibers. Consequently the element of  $K_3\mathbb{Z}[\xi]$  given by  $-f$  is the same modulo torsion as the one given by  $f$ . Since  $S^1$  is odd dimensional and orientable the involution of ‘turning the Morse function upside down’, i.e. replacing  $f$  by  $-f$  acts as  $-t$  on the associated  $K_3\mathbb{Z}[\xi]$ -invariant. (See [5] for more details about this involution.)  $\square$

## Acknowledgements

We would like to thank M. Harris for teaching us about  $L$ -functions of number fields and D. Ruberman for insisting to us that our original computer computations of the Borel regulator map were inadequate. Also T. Goodwillie helped us considerably with his usual enlightened remarks.

## References

1. Bloch, S.: Higher regulators, algebraic  $K$ -theory, and zeta functions of elliptic curves, Irvine Lecture Notes (1978).
2. Beilinson, A. A.: Higher regulators and values of  $L$ -functions, *Sovrem. Probl. Mat.* **24**, Viniti, Moscow (1984). Translation in *J. Soviet. Math.* **30** (1985), 2036–2070.

3. Cerf, J.: La stratification naturelle des espaces de fonctions différentiables réelles et le théorème de la pseudo-isotopie, *I.H.E.S. Publ. Math.* **39** (1970), 5–173.
4. Esnault, H.: On the Loday Symbol in Deligne–Beilinson Cohomology, *K-Theory* **3** (1989), 1–28.
5. Hsiang, W.-C.: On  $\pi_1(\text{Diff}(M^n))$ , in J. Cantrell (ed), *Geometric Topology*, Academic Press, New York, 1979, pp. 351–365.
6. Hatcher, A. and Wagoner, J.: Pseudo-isotopies of compact manifolds, *Astérisque* **6** (1973).
7. Igusa, K.: The  $\text{Wh}_3(\pi)$  obstruction for pseudoisotopy, PhD Thesis, Princeton University, 1979.
8. Igusa, K.: On the homotopy type of the space of generalized Morse functions, *Topology* **23** (1984), 245–256.
9. Igusa, K.: The stability theorem for smooth pseudoisotopies, *K-Theory* **2** (1988), 1–355.
10. Igusa, K. and Klein, J.: Filtered chain complexes and higher Franz–Reidemeister torsion, in preparation.
11. Klein, J.: The cell complex construction and higher  $R$ -torsion for bundles with framed Morse function, PhD. Thesis, Brandeis University, 1989.
12. Klein, J.: Parametrized Morse theory and higher Franz–Reidemeister torsion, preprint, Universität GH-Siegen (1991).
13. Lee, R. and Szczarba, R.: The group  $K_3(\mathbb{Z})$  is cyclic of order forty-eight, *Ann. Math. (2)* **104** (1976), 31–60.
14. Neukirch, J.: The Beilinson conjecture for algebraic number fields, in *Beilinson's Conjectures on Special Values of L-Functions*, Perspectives in Math. 4, Academic Press, New York, 1988, pp. 193–247.
15. Ramakrishnan, D.: Regulators, algebraic cycles, values of  $L$ -functions, *Algebraic K-Theory and Algebraic Number Theory*, Contemp. Math. Vol. 83, 1988, pp. 183–310.
16. Soulé, C.: Eléments cyclotomique en  $K$ -théorie, *Astérisque* **147–148** (1987), 225–257.



.....

